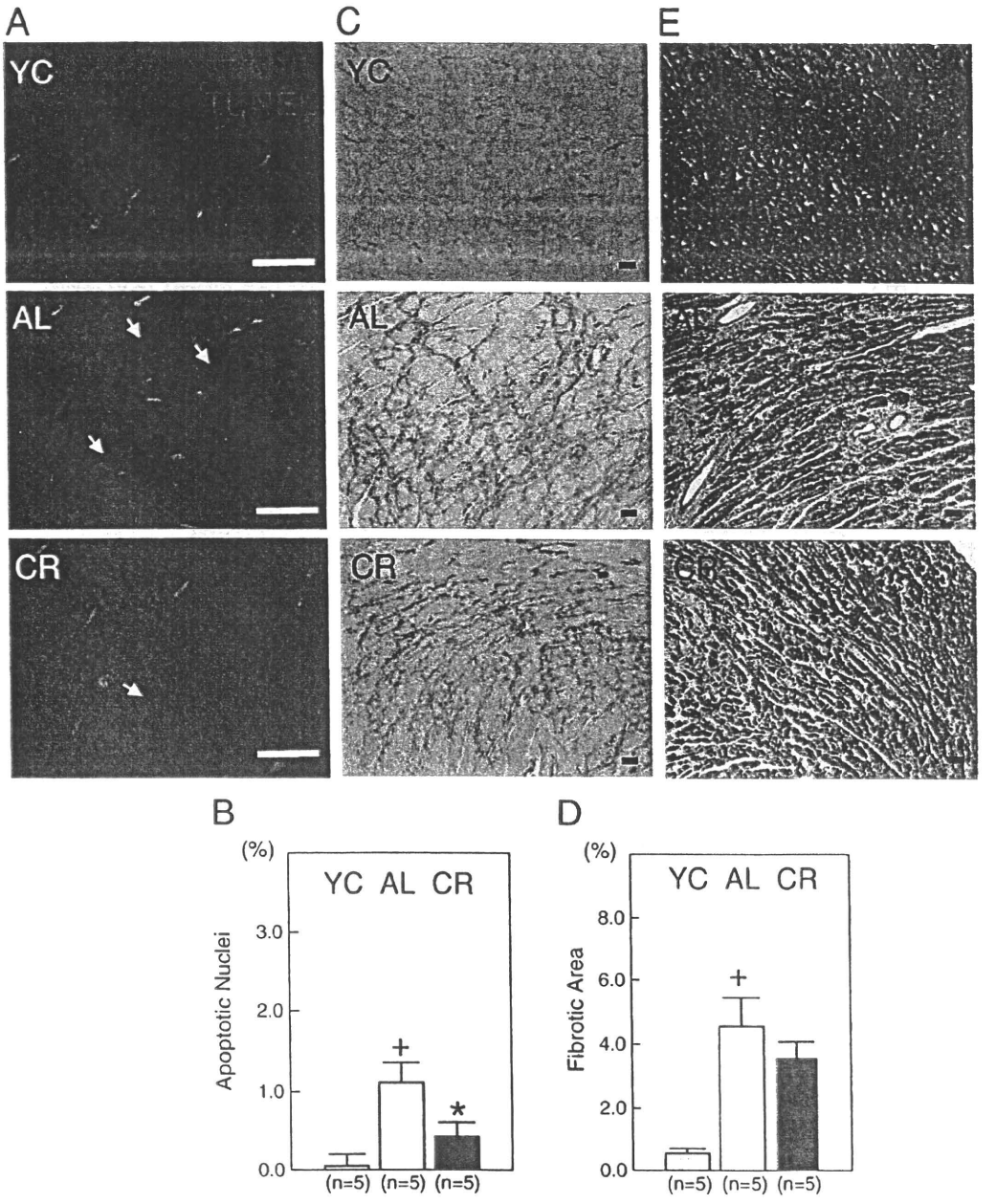

Fig. 2. Histological examination. (A) TUNEL staining. (B) Percentage of TUNEL-positive nuclei to total nuclei in AL and CR rats. (C) Picrosirius red staining. (D) Percentage of fibrotic area to LV area in AL and CR rats calculated in Picrosirius red staining. (E) Masson's trichrome staining. Bar: 50 μm. Data are the mean ± SEM. Quantitative data are pooled data from 5 AL hearts and 5 CR hearts. $^{+}P<0.05$ vs. the YC group. $^{*}P<0.05$ vs. the AL group.

in SERCA2 protein expression, but had no effect on the expression of NCX1 and phosphorylated and total PLB (Figs. 4(B and E)), both of which are involved in Ca^{2+} uptake during myocyte relaxation.

The amount of conjugated LC3 (LC3-II) correlates with the number of autophagosomes. More recently, it was reported that an increase in the ratio of LC3-II to the cytosolic form of LC3 (LC3-I) is a better biochemical marker by which to assess ongoing autophagy [22]. The expression levels of LC3-II and the LC3-II/LC3-I ratio decreased with aging (Figs. 5(A–C)). Although the expression levels of LC3-I were similar between AL and CR, the expression of LC3-II was significantly higher in hearts from CR rats, consequently increasing the ratio of LC3-II to LC3-I comparable with that in young hearts (Figs. 5(A–C)). In addition, the expression levels of beclin1 were higher in hearts from CR rats compared with that in hearts from AL rats (Figs. 5(A and D)).

To examine the possible involvement of the mTOR pathway as an upstream signaling of enhanced autophagy, the expression levels of phosphorylated and total mTOR and S6K were compared among three groups. There was no difference in the expression levels of phosphorylated and total mTOR and S6K between young and aged hearts (Fig. 6). However, long-term CR significantly attenuated phosphorylated forms of mTOR and S6K without affecting total protein levels (Fig. 6).

To clarify which mechanism is mainly responsible for the increase in LC3-II expression in the CR group, enhanced autophagic influx or lysosomal dysfunction, we evaluated the effects of chloroquine on the expression of LC3-II using male 20-month-old rats fed with either AL or CR for 12 months (Fig. 7). Because autophagic activity is represented by the flux in autophagosomes, this can be estimated by comparing LC3-II expression in the presence of the lysosomal protease inhibitor chloroquine [23]. Chloroquine treatment resulted

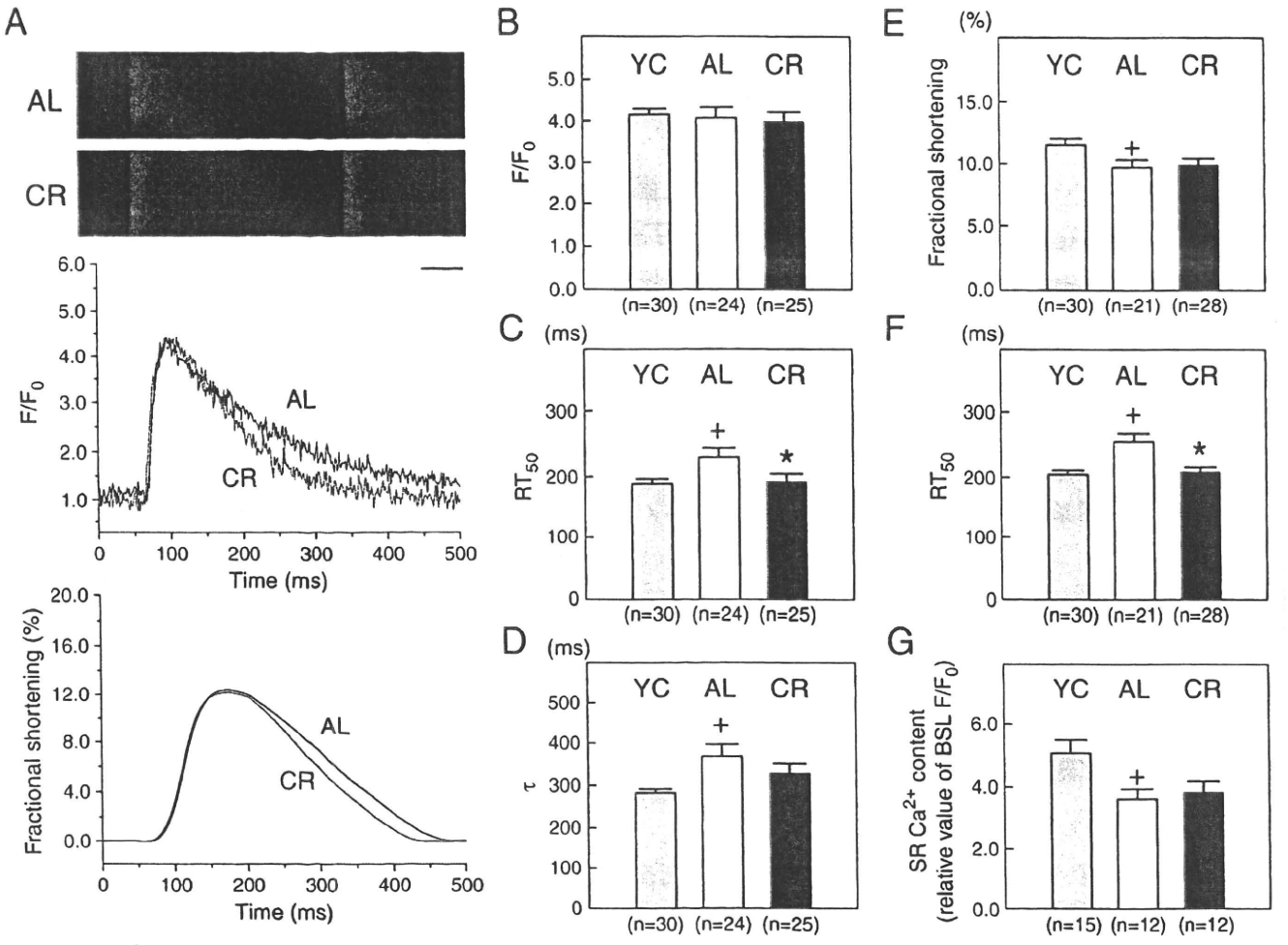

Fig. 3. Measurement of $[Ca^{2+}]_i$ and myocyte contractions in isolated myocytes. (A) Representative Fluo-4 line scan images and traces of Ca^{2+} transients and myocyte contractions in isolated myocytes obtained from AL and CR rats. (B) Ratio of peak to basal $[Ca^{2+}]_i$ amplitude, expressed as F/F_0. (C) Time to 50% relaxation in Ca^{2+} transient (RT_{50}). (D) τ of $[Ca^{2+}]_i$ decline. (E) Fractional shortening. (F) Time to 50% relaxation in myocyte contraction (RT_{50}). (G) SR Ca^{2+} content. Data are the mean ± SEM. $^{+}P<0.05$ vs. the YC group. $^{*}P<0.05$ vs. the AL group.

in a significant increase in LC3-II expression in both the AL and CR groups. However, the LC3-II/LC3-I ratio remained higher in hearts from CR rats compared with AL rats, suggesting that autophagic flux is enhanced in hearts from CR rats.

4. Discussion

The major findings of the present study are: (1) long-term CR improves LV diastolic function without affecting LV systolic function; (2) long-term CR attenuates myocyte apoptosis and the cardiac expression of markers of senescence, such as β-galactosidase, lipofuscin, and $p16^{INK4a}$; (3) long-term CR fails to reduce cardiac fibrosis and to prevent decreases in p-troponin I and p-phospolamban; (4) long-term CR attenuates the decrease in SERCA2 protein and ameliorates age-associated deterioration of intracellular Ca^{2+} handling; (5) long-term CR suppresses the mTOR pathway; and (6) long-term CR enhances autophagic flux in the heart.

The impact of long-term CR on cardiovascular senescence has not been fully evaluated. Taffet et al. reported that long-term CR improved age-associated changes in late diastolic function in mice [24]. More recently, Barger et al. demonstrated that CR prevents the age-related increase in isovolumic relaxation time and the decrease in the myocardial performance index in mice [25]. In the present study, long-term CR improved LV diastolic function without affecting LV systolic function in senescent rats. Furthermore, our results suggest that long-term CR ameliorates the age-associated deterioration of early diastolic function by maintaining the function of the sarcoplasmic reticulum (SR). Our findings differ from those of Taffet et al. [24] because those authors found no improvement in early diastolic cardiac function in mice. However, our results are consistent with those of Seymour et al. [26], who reported that CR improves cardiac remodeling and diastolic dysfunction in Dahl-SS rats.

The age-associated impairment in cardiac diastolic function is complicated. There is ample evidence from studies using senescent rats implicating slowed cardiac relaxation and altered Ca^{2+} handling in the impaired diastolic function [5,6,21]. In particular, impaired SERCA activity, which is mainly responsible for controlling $[Ca^{2+}]_i$ by taking up Ca^{2+} into the SR during relaxation, has been identified as contributing to the abnormalities in cardiac relaxation. The decrease in SR Ca^{2+} uptake during relaxation, which results in prolonged contraction, has been shown to be associated with decreased SERCA2 content and activity in experimental models of senescence [5,6,21]. More recently, SERCA2a protein levels have been reported to be significantly decreased in the senescent human myocardium [27]. Changes in active cardiac relaxation impact on early diastolic parameters, such as peak E velocity and E deceleration time, rather than on late diastolic parameters [28]. In the present study, attenuation of the decrease in SERCA2 protein and its activity in senescent CR hearts was associated with an improvement in RT_{50} and τ, indicators of a decline in $[Ca^{2+}]_i$. Schmidt et al. [21] demonstrated that overexpression of SERCA2a by gene transfer improved diastolic function in senescent rat hearts. Therefore, we speculate that long-

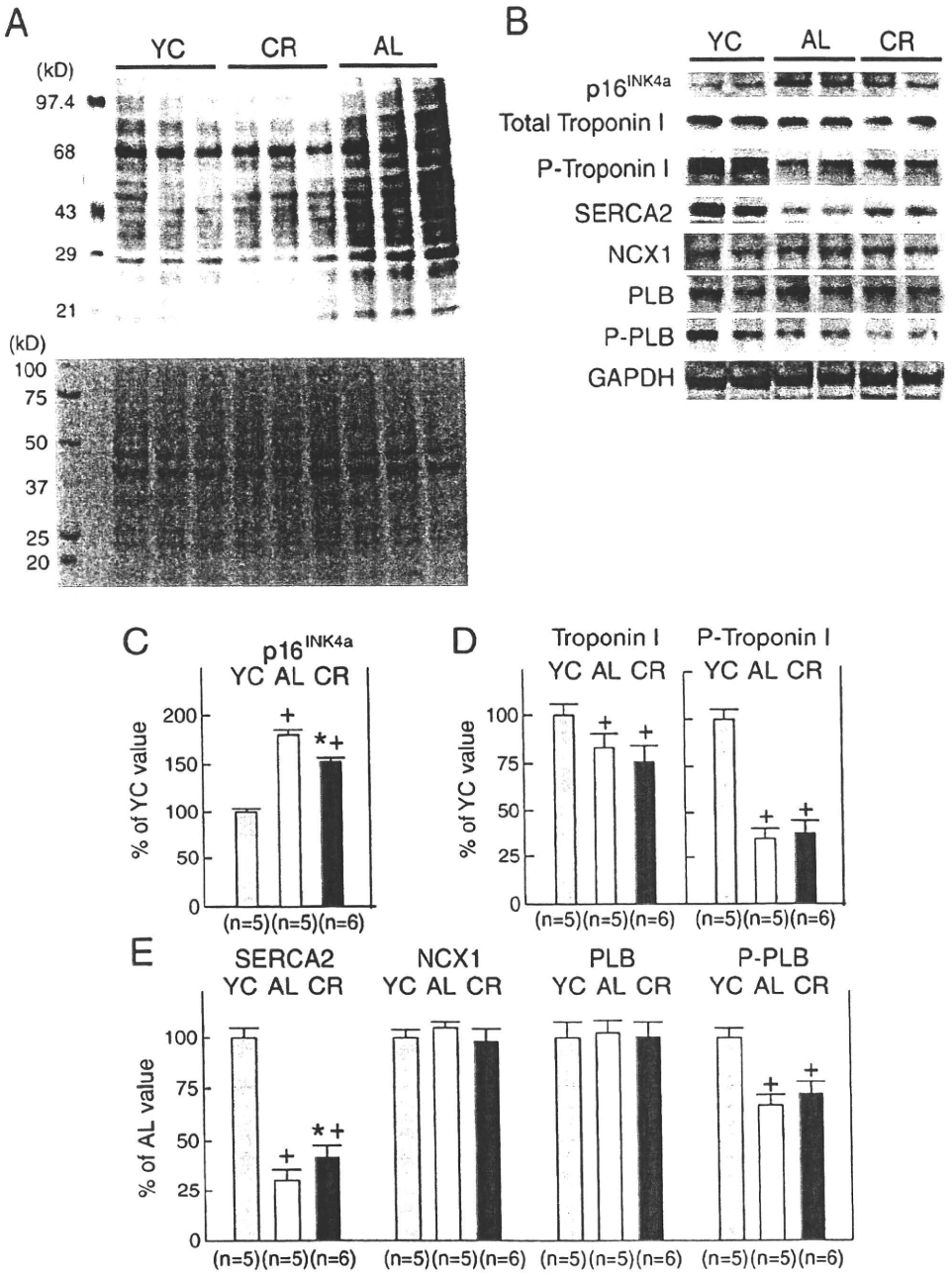

Fig. 4. Oxyblots and Western immunoblotting for senescence markers and proteins related to Ca^{2+} uptake during relaxation. (A) Representative oxyblots showing protein carbonyls (upper panel) and the corresponding Ponceau S staining (lower panel). (B) Representative Western immunoblots showing the expression of $p16^{INK4a}$, total troponin I, troponin I phosphorylated at the $Ser^{23/24}$ residue (P-troponin I), sarcoplasmic reticulum calcium ATPase (SERCA) 2, Na^+-Ca^{2+} exchanger (NCX) 1, total phospholamban (PLB), phospholamban phosphorylated at the Ser^{16} residue (P-PLB), and glyceraldehydes 3-phosphate dehydrogenase (GAPDH). (C) Densitometric analysis of $p16^{INK4a}$. (D) Densitometric analysis of total troponin I and P-troponin I. (E) Densitometric analysis of SERCA2, NCX1, total PLB and P-PLB. Densitometric measurements of protein immunoreactivity are expressed as a percentage of the average value measured in YC rats. Data are the mean ± SEM. $^+P<0.05$ vs. the YC group. $^*P<0.05$ vs. the AL group. YC: young controls.

term CR ameliorates the age-associated deterioration of myocyte relaxation by attenuating the decrease in SERCA2 protein with aging.

It was demonstrated recently that mice with cardiac-specific excision of the SERCA2 gene present only moderate contractile dysfunction because of an SR-independent compensatory mechanism [18]. These results might argue against a major role of SERCA2 for diastolic dysfunction. Similarly, enhanced SERCA2 activity is usually associated with enhanced Ca^{2+} transient and contractility [29]. However, these findings were not consistent with our results. In contrast to cardiac-specific SERCA2-deficient mice, the decrease in SERCA2 proteins might develop very slowly in aged rats. The induction of cardiomyocyte-specific *Serca2* gene excision resulted in less than 5% SERCA2 protein expression [18], although the expression levels of SERCA2 protein in the AL aged heart remained at 30% of levels in the young heart (Fig. 4(E)). Thus, based on the results of Anderson et al. [18], we propose that the change in SERCA2 expression impacted markedly on myocyte Ca^{2+} homeostasis so the compensatory mechanism was strongly invoked in cardiomyocyte-specific *Serca2*-deficient mice. As shown in Figs. 3 and 4, there was no difference in peak Ca^{2+} transient or in expression levels of Na^+-Ca^{2+} exchanger between the AL and CR hearts, suggesting that the compensatory mechanism regarding SR Ca^{2+} handling was not sufficiently evoked in

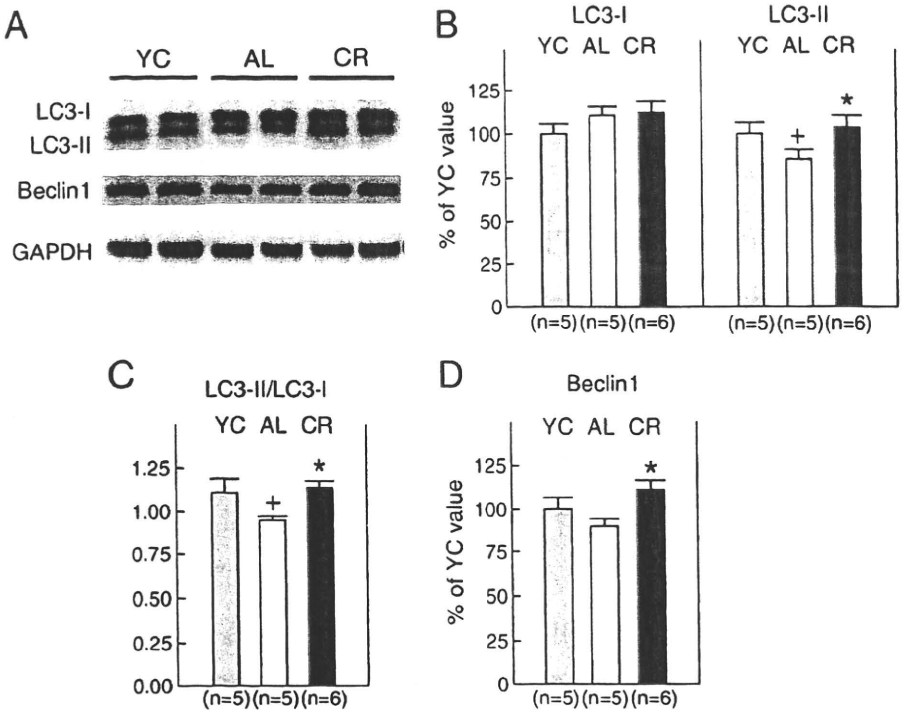

Fig. 5. Western immunoblotting for light chain 3 (LC3) and beclin1. (A) Representative Western immunoblots showing the expression of conjugated (LC3-II), cytosolic (LC3-I) LC3, beclin1 and GAPDH. (B) Densitometric analysis of LC3-I and LC3-II. (C) The LC3-II/LC3-I ratio. (D) Densitometric analysis of beclin1. Densitometric measurements of protein immunoreactivity are expressed as a percentage of the average value measured in YC rats. Data are the mean ± SEM. $^{+}P<0.05$ vs. the YC group. $^{*}P<0.05$ vs. the AL group. YC: young controls.

the aged heart. Although CR enhanced SERCA2 protein expression and activity in the aged heart, there was no difference in the SR Ca^{2+} content between myocytes obtained from the AL and CR hearts. Overall, we speculate that CR could improve SR Ca^{2+} uptake rate during myocyte relaxation, but would not impact sufficiently to increase total SR Ca^{2+} content because the magnitude of the increase

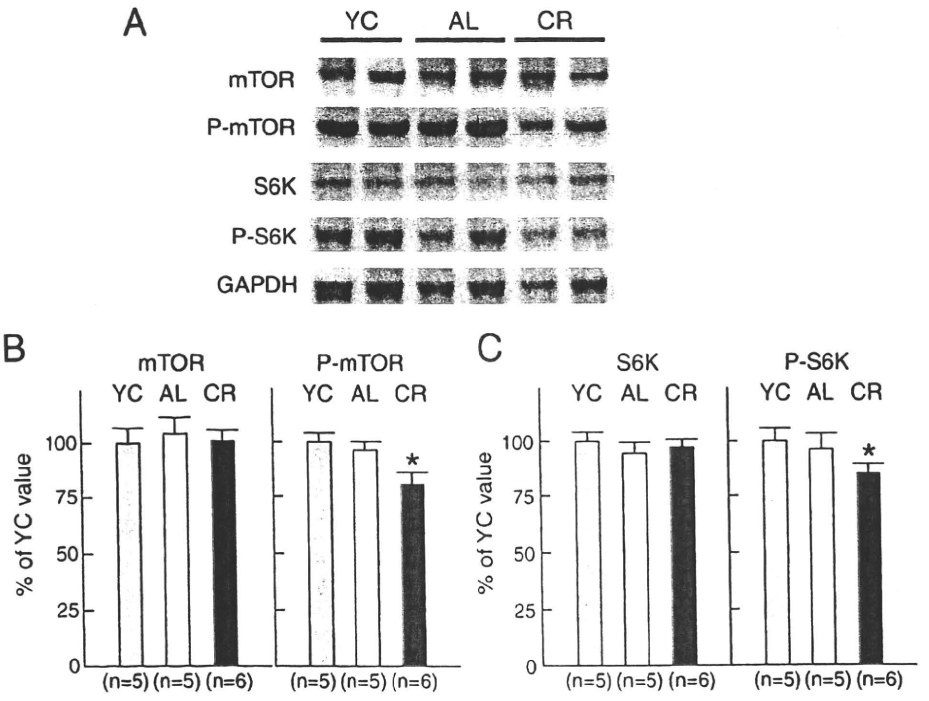

Fig. 6. Western immunoblotting for mammalian target of rapamycin (mTOR) signalings. (A) Representative Western immunoblots showing the expression of total mTOR, mTOR phosphorylated at the Ser^{2448} residue (P-mTOR), total p70 S6 kinase (S6K), S6K phosphorylated at the Thr^{389} residue (P-S6K) and GAPDH. (B) Densitometric analysis of total mTOR and P-mTOR. (C) Densitometric analysis of total S6K and P-S6K. Densitometric measurements of protein immunoreactivity are expressed as a percentage of the average value measured in YC rats. Data are the mean ± SEM. $^{*}P<0.05$ vs. the AL group. YC: young controls.

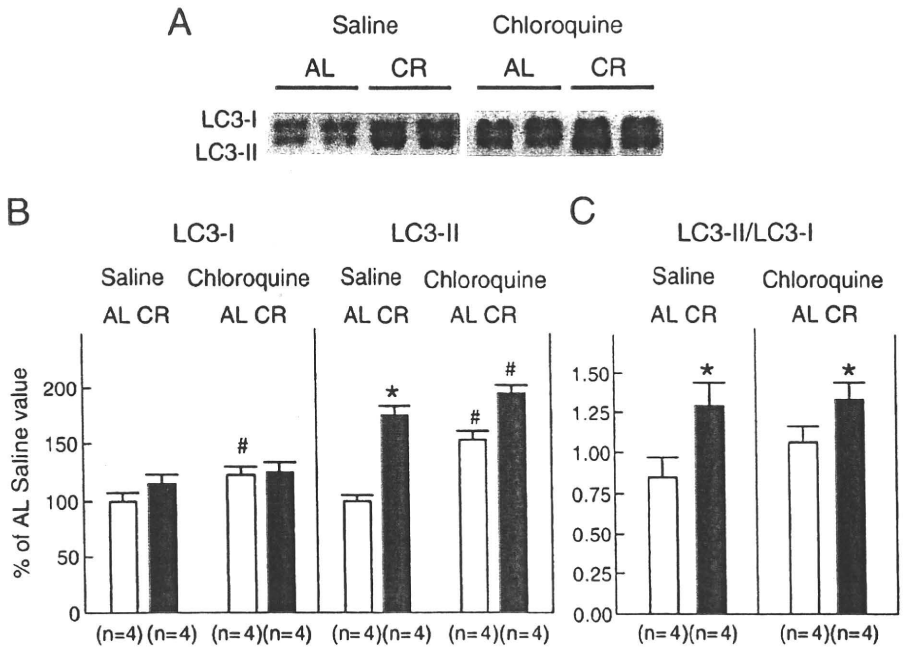

Fig. 7. Western immunoblotting for LC3 in 20-month-old AL and CR rats treated with either saline or chloroquine. (A) Representative Western immunoblots showing the expression of LC3-I and LC3-II. (B) Densitometric analysis of LC3-I and LC3-II. (C) The LC3-II/LC3-I ratio. Densitometric measurements of protein immunoreactivity are expressed as a percentage of the average value in AL rats treated with saline. Data are the mean ± SEM. *P<0.05 vs. the AL group; #P<0.05 vs. the corresponding saline-treated group.

in SERCA2 protein by CR was only slight compared with previous reports in which SERCA2 was overexpressed in the failing human heart [29] and the senescent rat heart [21]. Therefore, enhanced SERCA2 protein expression by CR was not associated with enhanced Ca^{2+} transient and contractility in the present study.

In addition, decreased size of cardiomyocytes might contribute to the amelioration of LV diastolic dysfunction in CR rats. Myocyte hypertrophy is associated with changes in the cytoskeletal proteins that could alter the microtubule architecture and heighten organization of sarcomeres within individual myocytes. An increased collagen volume fraction, larger cardiomyocyte diameter, and higher resting cardiomyocyte tension have been correlated with LV diastolic stiffness [30]. With aging, the myosin heavy chain isoform shifts from α to β in the rodent heart [5]. Lieber et al. [31] demonstrated that α- and β-tubulin were significantly increased and desmin was decreased in aged rats, and this finding might explain the observed cardiac dysfunction with aging. Posttranslational modification of myofilament proteins including titin might play an important role in diastolic heart failure associated with aging [32]. Our results indicated that cardiomyocyte responsiveness to Ca^{2+} estimated from the relationship between Ca^{2+} transient and myocyte shortening is similar between isolated myocytes obtained from AL and CR rat hearts (Fig. 3). This finding supports our hypothesis that inhibiting the SERCA2 expression decline is a major factor in preserving LV diastolic function by CR. However, it is also possible that CR affects these age-associated alterations in cytoskeletal proteins. Thus, we would evaluate the changes in myofilament proteins in aged rats treated with long-term CR in future studies.

The accumulation of myocardial collagen and extracellular matrix increases with aging, contributing to increased cardiac fibrosis, myocardial stiffness, and cardiac diastolic dysfunction [5,6]. Dhahbi et al. demonstrated that long-term CR reduced myocardial collagen and extracellular matrix content and attenuated cardiac fibrosis associated with aging [33]. Thus, CR-induced changes in cardiac connective tissue may contribute, in part, to the amelioration of diastolic function, especially late diastolic function, as observed by Taffet et al. [24]. However, we could not find a significant decrease in cardiac fibrosis in CR rat hearts (Figs. 2(C–E)). We speculate that the discrepancy between the study of Taffet et al. [24] and the present study could be due, at least in part, to species differences and large individual variations with physiological aging. In addition, this discrepancy could be related to species functional differences including the metabolic rate and heart rate. These differences must be considered with regard to fibrosis, extracellular matrix composition, and fibrosis–renin–angiotensin–aldosterone system (RAS) interactions. Recent investigations revealed an essential role of RAS on the development of cardiac fibrosis with aging. Both pharmacological inhibition of RAS and targeted disruption of the angiotensin type 1 receptor prolonged lifespan and significantly attenuated cardiac fibrosis associated with aging [34,35]. Thus, our results may suggest that CR is not sufficient to suppress the activation of RAS with aging. Further investigations are necessary to clarify this issue.

The mechanisms by which long-term CR retards cellular senescence and attenuates the physiological decline of organ function have not been fully elucidated. Aging occurs, in part, as a result of the accumulation of oxidative damage caused by oxidative free radicals that are generated continuously during the course of metabolic processes [5,6,8]. In contrast, CR decreases the age-associated accumulation of oxidative damage to lipids, proteins, and DNA [7,8,26]. In the present study, the expression of protein carbonyls was less in CR hearts compared with AL hearts (Fig. 4A). Thus, it is possible that long-term CR retards cellular senescence and ameliorates age-related functional decline by attenuating oxidative damage in the aged heart. However, there is still no direct evidence that attenuation of oxidative damage is the primary means by which CR prevents cardiac senescence.

Another possible mechanism by which long-term CR retards cardiac senescence is enhancement of autophagy. Although the role of autophagy under stressed conditions is yet to be elucidated, autophagy under basal conditions plays a housekeeping role in the turnover of cytoplasmic constituents [22,23]. Thus, enhanced autophagy during CR is considered to be protective by degrading and removing damaged organelles and accumulated protein

aggregates. Our results indicate that autophagic flux is enhanced in CR hearts and this finding is consistent with previous studies [36]. Inuzuka et al. demonstrated that suppression of phosphoinositide 3-kinase preserved cardiac function and attenuated the expression of senescence makers associated with enhanced autophagy [14]. Temporal inhibition of autophagy in tamoxifen-treated $Atg5^{flox/flox}$; $MerCreMer^{+}$ mice leads to LV hypertrophy, LV dilatation, and contractile dysfunction [37]. Because autophagy is not inhibited but is only somewhat imperfect in the aged heart [38], the accumulation of impaired SR and mitochondria is sublethal and may result in diastolic dysfunction only. Impaired autophagy in the aged heart may contribute, in part, to the accumulation of lipofuscin, further inhibiting autophagy [38]. In the present study, long-term CR attenuated the accumulation of lipofuscin, suggesting that long-term CR disrupts this cycle in the aged heart. In addition, we demonstrated that enhanced autophagy was associated with suppressed the mTOR pathway in the hearts. Activation of mTOR exerts a negative regulatory effect on the induction of autophagy [39]. Rapamycin, an inhibitor of mTOR, has been shown to regress existing cardiac hypertrophy induced by pressure overload [40] and, more recently, has been reported to prolong lifespan in mice if it was started after middle age [41]. However, the exact mechanism by which enhanced autophagy preserves LV diastolic function remains to be resolved in the future. Further studies are also necessary to determine the upstream pathways of mTOR such as AMP-activated protein kinase and phosphoinositide 3-kinase/Akt in CR hearts.

Meyer et al. demonstrated that CR was beneficial for LV diastolic function in humans, because the E/A ratio was greater in their CR group than in the group fed a Western diet, with no significant differences in LV systolic function between them [11]. Meyer et al. speculated that CR has a beneficial effect on LV diastolic function by lowering systolic blood pressure and decreasing systemic inflammation and probably myocardial fibrosis. Although it is difficult to compare the data from human studies with those obtained in experimental animal models, it seems reasonable to assume that a common mechanism is involved in CR-induced improvements in LV diastolic function. Recent investigations suggest that myocardial triglyceride content is an independent predictor of diastolic function in the elderly [42] and patients with T2DM [43]. The decrease in myocardial triglyceride content produced by CR was associated with an improvement in LV diastolic function [13]. It is plausible that enhanced autophagy contributes to the degradation of potentially toxic fatty acid intermediates.

In conclusion, the present study has demonstrated that long-term CR partially retards cardiac senescence and attenuates the functional decline of the aged heart. Because the increased incidence of CHF in the elderly is becoming an urgent health problem in developed countries [2], CR and CR mimetics may provide a novel therapeutic strategy for reducing patients with LV diastolic dysfunction. Although we cannot yet conclude that there is a common mechanism underlying the effects of CR in humans and animal experimental models, the results of the present study do suggest the usefulness of enhanced autophagy as a novel therapeutic strategy to maintain cardiac diastolic function.

Supplementary materials related to this article can be found online at doi:10.1016/j.yjmcc.2010.10.018.

Acknowledgments

The authors thank Drs. Roberto Bolli and Shin-ichiro Imai for critical discussions and Mr. Yoshiharu Tsuru, Ms. Yoshiko Miyake, and Ms. Naoko Higashijima for their technical assistance.

This study was supported in part by the Vehicle Racing Commemorative Foundation (2007–2009) (to Dr. Shinmura and Dr. Sano), by the Nateglinide Memorial Toyoshima Research and Education Fund (2007), and by the Novartis Foundation for Gerontological Research (2008) (to Dr. Shinmura). There is no relationship with industry.

References

[1] Haan MN, Selby JV, Quesenberry Jr CP, Schmittdiel JA, Fireman BH, Rice DP. The impact of aging and chronic disease on use of hospital and outpatient services in a large HMO: 1971–1991. J Am Geriatr Soc 1997;45:667–74.
[2] Lakatta EG, Levy D. Arterial and cardiac aging: major shareholders in cardiovascular disease enterprises: part II: the aging heart in health: links to heart disease. Circulation 2003;107:346–54.
[3] Chatterjee K, Massie B. Systolic and diastolic heart failure: differences and similarities. J Card Fail 2007;13:569–76.
[4] Boluyt MO, Converso K, Hwang HS, Mikkor A, Russell MW. Echocardiographic assessment of age-associated changes in systolic and diastolic function of the female F344 rat heart. J Appl Physiol 2004;96:822–8.
[5] Lakatta EG. Arterial and cardiac aging: major shareholders in cardiovascular disease enterprises: part III: cellular and molecular clues to heart and arterial aging. Circulation 2003;107:490–7.
[6] Weisfeldt M. Aging, changes in the cardiovascular system, and responses to stress. Am J Hypertens 1998;11:41S–5S.
[7] Heilbronn LK, Ravussin E. Calorie restriction and aging: review of the literature and implications for studies in humans. Am J Clin Nutr 2003;78:361–9.
[8] Masoro EJ. Overview of caloric restriction and ageing. Mech Ageing Dev 2005;126: 913–22.
[9] Shinmura K, Tamaki K, Bolli R. Short-term caloric restriction improves ischemic tolerance independent of opening of ATP-sensitive K+ channels in both young and aged hearts. J Mol Cell Cardiol 2005;39:285–96.
[10] Shinmura K, Tamaki K, Bolli R. Impact of 6-mo caloric restriction on myocardial ischemic tolerance: possible involvement of nitric oxide-dependent increase in nuclear Sirt1. Am J Physiol Heart Circ Physiol 2008;295:H2348–55.
[11] Meyer TE, Kovacs SJ, Ehsani AA, Klein S, Holloszy JO, Fontana L. Long-term caloric restriction ameliorates the decline in diastolic function in humans. J Am Coll Cardiol 2006;47:398–402.
[12] Riordan MM, Weiss EP, Meyer TE, Ehsani AA, Racette SB, Villareal DT, et al. The effects of caloric restriction- and exercise-induced weight loss on left ventricular diastolic function. Am J Physiol Heart Circ Physiol 2008;294:H1174–82.
[13] Hammer S, Snel M, Lamb HJ, Jazet IM, van der Meer RW, Pijl H, et al. Prolonged caloric restriction in obese patients with type 2 diabetes mellitus decreases myocardial triglyceride content and improves myocardial function. J Am Coll Cardiol 2008;52:1006–12.
[14] Inuzuka Y, Okuda J, Kawashima T, Kato T, Niizuma S, Tamaki Y, et al. Suppression of phosphoinositide 3-kinase prevents cardiac aging in mice. Circulation 2009;120:1695–703.
[15] Savitha S, Naveen B, Panneerselvam C. Carnitine and lipoate ameliorates lipofuscin accumulation and monoamine oxidase activity in aged rat heart. Eur J Pharmacol 2007;574:61–5.
[16] Ishida H, Genka C, Hirota Y, Nakazawa H, Barry WH. Formation of planar and spiral Ca2+ waves in isolated cardiac myocytes. Biophys J 1999;77:2114–22.
[17] Picht E, DeSantiago J, Huke S, Kaetzel MA, Dedman JR, Bers DM. CaMKII inhibition targeted to the sarcoplasmic reticulum inhibits frequency-dependent acceleration of relaxation and Ca2+ current facilitation. J Mol Cell Cardiol 2007;42: 196–205.
[18] Andersson KB, Birkeland JA, Finsen AV, Louch WE, Sjaastad I, Wang Y, et al. Moderate heart dysfunction in mice with inducible cardiomyocyte-specific excision of the Serca2 gene. J Mol Cell Cardiol 2009;47:180–7.
[19] Hajjar RJ, Kang JX, Gwathmey JK, Rosenzweig A. Physiological effects of adenoviral gene transfer of sarcoplasmic reticulum calcium ATPase in isolated rat myocytes. Circulation 1997;95:423–9.
[20] Divald A, Kivity S, Wang P, Hochhauser E, Roberts B, Teichberg S, Gomes AV, Powell SR. Myocardial ischemic preconditioning preserves postischemic function of the 26S proteasome through diminished oxidative damage to 19S regulatory particle subunits. Circ Res 2010;106:1829–38.
[21] Schmidt U, del Monte F, Miyamoto MI, Matsui T, Gwathmey JK, Rosenzweig A, et al. Restoration of diastolic function in senescent rat hearts through adenoviral gene transfer of sarcoplasmic reticulum Ca(2+)-ATPase. Circulation 2000;101: 790–6.
[22] Mizushima N, Yoshimori T. How to interpret LC3 immunoblotting. Autophagy 2007;3:542–5.
[23] Iwai-Kanai E, Yuan H, Huang C, Sayen MR, Perry-Garza CN, Kim L, et al. A method to measure cardiac autophagic flux in vivo. Autophagy 2008;4:322–9.
[24] Taffet GE, Pham TT, Hartley CJ. The age-associated alterations in late diastolic function in mice are improved by caloric restriction. J Gerontol A Biol Sci Med Sci 1997;52:B285–90.
[25] Barger JL, Kayo T, Vann JM, Arias EB, Wang J, Hacker TA, et al. A low dose of dietary resveratrol partially mimics caloric restriction and retards aging parameters in mice. PLoS ONE 2008;3:e2264.
[26] Seymour EM, Parikh RV, Singer AA, Bolling SF. Moderate calorie restriction improves cardiac remodeling and diastolic dysfunction in the Dahl-SS rat. J Mol Cell Cardiol 2006;41:661–8.
[27] Cain BS, Meldrum DR, Joo KS, Wang JF, Meng X, Cleveland Jr JC, et al. Human SERCA2a levels correlate inversely with age in senescent human myocardium. J Am Coll Cardiol 1998;32:458–67.
[28] Nishimura RA, Abel MD, Hatle LK, Holmes Jr DR, Housmans PR, Ritman EL, et al. Significance of Doppler indices of diastolic filling of the left ventricle: comparison with invasive hemodynamics in a canine model. Am Heart J 1989;118:1248–58.
[29] del Monte F, Harding SE, Schmidt U, Matsui T, Kang ZB, Dec GW, et al. Restoration of contractile function in isolated cardiomyocytes from failing human hearts by gene transfer of SERCA2a. Circulation 1999;100:2308–11.

[30] Borbely A, van der Velden J, Papp Z, Bronzwaer JG, Edes I, Stienen GJ, et al. Cardiomyocyte stiffness in diastolic heart failure. Circulation 2005;111:774–81.
[31] Lieber SC, Qiu H, Chen L, Shen YT, Hong C, Hunter WC, et al. Cardiac dysfunction in aging conscious rats: altered cardiac cytoskeletal proteins as a potential mechanism. Am J Physiol Heart Circ Physiol 2008;295:H860–6.
[32] Granzier H, Wu Y, Siegfried L, LeWinter M. Titin: physiological function and role in cardiomyopathy and failure. Heart Fail Rev 2005;10:211–23.
[33] Dhahbi JM, Tsuchiya T, Kim HJ, Mote PL, Spindler SR. Gene expression and physiologic responses of the heart to the initiation and withdrawal of caloric restriction. J Gerontol A Biol Sci Med Sci 2006;61:218–31.
[34] Basso N, Cini R, Pietrelli A, Ferder L, Terragno NA, Inserra F. Protective effect of long-term angiotensin II inhibition. Am J Physiol Heart Circ Physiol 2007;293: H1351–8.
[35] Benigni A, Corna D, Zoja C, Sonzogni A, Latini R, Salio M, et al. Disruption of the Ang II type 1 receptor promotes longevity in mice. J Clin Invest 2009;119: 524–30.
[36] Wohlgemuth SE, Julian D, Akin DE, Fried J, Toscano K, Leeuwenburgh C, et al. Autophagy in the heart and liver during normal aging and calorie restriction. Rejuvenation Res 2007;10:281–92.
[37] Nakai A, Yamaguchi O, Takeda T, Higuchi Y, Hikoso S, Taniike M, et al. The role of autophagy in cardiomyocytes in the basal state and in response to hemodynamic stress. Nat Med 2007;13:619–24.
[38] Terman A, Brunk UT. Autophagy in cardiac myocyte homeostasis, aging, and pathology. Cardiovasc Res 2005;68:355–65.
[39] Gottlieb RA, Carreira RS. Autophagy in health and disease. 5. Mitophagy as a way of life. Am J Physiol Cell Physiol 2010;299:C203–10.
[40] McMullen JR, Sherwood MC, Tarnavski O, Zhang L, Dorfman AL, Shioi T, et al. Inhibition of mTOR signaling with rapamycin regresses established cardiac hypertrophy induced by pressure overload. Circulation 2004;109:3050–5.
[41] Harrison DE, Strong R, Sharp ZD, Nelson JF, Astle CM, Flurkey K, et al. Rapamycin fed late in life extends lifespan in genetically heterogeneous mice. Nature 2009;460: 392–5.
[42] van der Meer RW, Rijzewijk LJ, Diamant M, Hammer S, Schar M, Bax JJ, et al. The ageing male heart: myocardial triglyceride content as independent predictor of diastolic function. Eur Heart J 2008;29:1516–22.
[43] Rijzewijk LJ, van der Meer RW, Smit JW, Diamant M, Bax JJ, Hammer S, et al. Myocardial steatosis is an independent predictor of diastolic dysfunction in type 2 diabetes mellitus. J Am Coll Cardiol 2008;52:1793–9.

Neural Crest–Derived Stem Cells Migrate and Differentiate Into Cardiomyocytes After Myocardial Infarction

Yuichi Tamura, Keisuke Matsumura, Motoaki Sano, Hidenori Tabata, Kensuke Kimura, Masaki Ieda, Takahide Arai, Yohei Ohno, Hideaki Kanazawa, Shinsuke Yuasa, Ruri Kaneda, Shinji Makino, Kazunori Nakajima, Hideyuki Okano, Keiichi Fukuda

Objective—We recently demonstrated that primitive neural crest–derived (NC) cells migrate from the cardiac neural crest during embryonic development and remain in the heart as dormant stem cells, with the capacity to differentiate into various cell types, including cardiomyocytes. Here, we examined the migration and differentiation potential of these cells on myocardial infarction (MI).

Methods and Results—We obtained double-transgenic mice by crossing protein-0 promoter-Cre mice with Floxed–enhanced green fluorescent protein mice, in which the NC cells express enhanced green fluorescent protein. In the neonatal heart, NC stem cells (NCSCs) were localized predominantly in the outflow tract, but they were also distributed in a gradient from base to apex throughout the ventricular myocardium. Time-lapse video analysis revealed that the NCSCs were migratory. Some NCSCs persisted in the adult heart. On MI, NCSCs accumulated at the ischemic border zone area (BZA), which expresses monocyte chemoattractant protein-1 (MCP-1). Ex vivo cell migration assays demonstrated that MCP-1 induced NCSC migration and that this chemotactic effect was significantly depressed by an anti-MCP-1 antibody. Small NC cardiomyocytes first appeared in the BZA 2 weeks post-MI and gradually increased in number thereafter.

Conclusion—These results suggested that NCSCs migrate into the BZA via MCP-1/CCR2 signaling and contribute to the provision of cardiomyocytes for cardiac regeneration after MI. (***Arterioscler Thromb Vasc Biol.* 2011;31:582-589.**)

Key Words: biology, developmental ■ cytokines ■ ischemic heart disease ■ molecular biology ■ cardiac regeneration

Several types of stem cells have been identified in adult heart, including c-Kit-positive, Sca-1-positive, Isl-1-positive, and side-population cells.[1–4] All of these can differentiate into various cell types, including cardiomyocytes. However, the developmental origins of these cardiac stem cells remain unclear.

Neural crest–derived (NC) cells constitute the fourth germ cell layer in the developing embryo. Cells from the neural crest are characterized by extensive migration and can differentiate in various developing tissues into neurons, glial cells, endocrine organs, bone, tooth, cartilage, pigmented epithelium, cornea, and aortic smooth muscle cells.[5–7] In addition, some NC cells are retained in the adult tissues as dormant stem cells, referred to as NC stem cells (NCSCs).[8–10]

We recently isolated the side-population cells from mammalian heart.[11] These cells formed a neurosphere-like structure that expressed nestin and Musashi-1, which is a marker of undifferentiated neural precursor cells[12] and could differentiate into neurons, glial cells, smooth muscle cells, and cardiomyocytes. Furthermore, when these sphere-forming cells were transplanted into the neural crest of a chick embryo, they migrated and differentiated into neurons and glial cells at the sympathetic ganglia, dorsal root ganglia, and spinal nerves. They also migrated into the developing heart region via the lateral pathway.[11] These results suggested the existence of a pool of NCSCs that are dormant in the adult myocardium. The regenerative potential of such a cell population in injured heart remains to be determined.

This study traced the fate of NC cells in heart during postneonatal growth and after myocardial infarction (MI) using double-transgenic (Tg) mice harboring protein-0 (P0) promoter-Cre[13] and Floxed–enhanced green fluorescent protein (EGFP).[14] The P0 glycoprotein was originally identified as a Schwann cell–specific myelin protein,[15] but it is also expressed in migrating neural crest cells during the early embryonic period in chicks.[16] In the double-Tg mice, transient activation of the P0 promoter induces Cre-mediated recombination, which tags subsets of the NC cells with

Received on: August 16, 2010; final version accepted on: December 9, 2010.

From the Departments of Cardiology (Y.T., K.M., M.S., K.K., M.I., T.A., Y.O., H.K., S.Y., R.K., S.M., K.F.), Anatomy (H.T., K.N.), and Physiology (H.O.), Keio University School of Medicine, Tokyo, Japan.

Drs Tamura and Matsumura contributed equally to this work.

Correspondence to Motoaki Sano, Department of Cardiology, Keio University School of Medicine, 35 Shinanomachi Shinjuku-ku, Tokyo 160-8582, Japan (E-mail msano@sc.itc.keio.ac.jp); or Keiichi Fukuda, Department of Cardiology, Keio University School of Medicine, 35 Shinanomachi Shinjuku-ku, Tokyo 160-8582, Japan (E-mail kfukuda@sc.itc.keio.ac.jp).

Arterioscler Thromb Vasc Biol is available at http://atvb.ahajournals.org DOI: 10.1161/ATVBAHA.110.214726

EGFP.[13,14,17] The EGFP-positive NCSCs were concentrated in the outflow tract, although they were also detected in the ventricular myocardium during the perinatal period. Time-lapse video analysis of living tissue from these mice revealed migratory NCSCs in the ventricular myocardium. EGFP-positive, NCSC-derived cardiomyocytes appeared during the postnatal period and increased in number as the heart grew. Although there was a corresponding decrease in the number of the EGFP-positive NCSCs as the heart grew, these cells persisted in the adult heart. On MI, the EGFP-positive NCSCs accumulated in the ischemic border zone area (BZA), which expresses monocyte chemoattractant protein-1 (MCP-1). Ex vivo cell migration assays demonstrated that this zonal MCP-1 gradient induced the migration of NCSCs, which then contributed to the regeneration of cardiomyocytes following injury.

Methods

Animals

The P0-Cre and plasminogen activator–Cre recombinase Tg mice were provided by K. Yamamura[13] and S. Dufour,[18] respectively. The Wnt-1-Cre recombinase Tg mice[19] were purchased from the Jackson Laboratory. The CAG-CAT-EGFP Tg mice were a gift from J. Miyazaki.[14] All experimental procedures and protocols were approved by the Animal Care and Use Committee of Keio University, Japan, and conformed to the National Institutes of Health Guide for the Care and Use of Laboratory Animals.

Flow Cytometry

Neonatal hearts from P0-cre/EGFP Tg mice were enzymatically digested in preparation for flow cytometry analysis. Cells were washed twice with phosphate-buffered saline (PBS) and then fixed with 2% paraformaldehyde for 10 minutes on ice. Cells were resuspended to a concentration of 10^6 cells/mL in PBS. In all experiments, 5×10^4 events were analyzed. To isolate EGFP-positive cells from the neonatal hearts, we adopted pseudo-2-dimensional separation using 2 band-pass filters, for green fluorescent protein (515 to 545 nm) and allophycocyanin (650 to 670 nm). By this method, autofluorescing nonstained cells were distributed on the diagonal line, whereas the EGFP-positive cells were localized above the diagonal line. We then sorted the EGFP-positive cells and confirmed their emission phenotype by fluorescence microscopy. The EGFP-positive cells were stained using mouse anti-nestin antibody (Abcam, 1:100), phycoerythrin-labeled rat anti-mouse CD117 (c-kit, BD Bioscience, 1:200), and phycoerythrin-labeled rat anti-mouse Ly-6A/E (Sca-1, BD Bioscience, 1:200). Alexa Fluor 594–conjugated donkey anti-mouse immunoglobulin (Molecular Probes, 1:500) was used as a secondary antibody to detect the anti-nestin antibody binding. Cell analysis and sorting were performed on a triple-laser BD FACSAria (Becton Dickinson).

Generation of MI

MI was generated as described previously.[20] Briefly, 8-week-old mice were lightly anesthetized with diethyl ether, intubated, and then fully anesthetized with 0.5% isoflurane gas while being mechanically ventilated with a Harvard respirator. A thoracotomy was then performed at the fourth intercostal space to expose the heart, and the left coronary artery was ligated at the mid–left ventricular level with 7-0 silk. The chest was then closed, and the mice were maintained under standard conditions. Control mice were subjected to sham operations. The mice were euthanized at 1, 2, 3, 4, 8, and 12 weeks postsurgery, and their hearts were isolated.

Histology and Immunostaining

Mice were euthanized using pentobarbital injection before perfusion of the hearts from the apex with PBS and perfusion fixing with 4% paraformaldehyde in PBS. The hearts were then dissected, cryoprotected in sucrose at 4°C, embedded in OCT compound (Miles Scientific), and snap-frozen in liquid nitrogen. The fixed-frozen heart tissue was sectioned (8-μm thickness) using a CM3050S cryostat (Leica) and short-axis sections at the mid-(left ventricle) level were stained with Azan. For immunostaining, sections were blocked in 5% bovine serum albumin for 30 minutes at room temperature and stained with anti-α-actinin (clone EA53, 1:800, Sigma), anti-GATA4 (N-19, 1:400, Santa Cruz Biotechnology), anti-connexin 43 (CX43, 1:400, Sigma), anti-nestin (Rat 401, 1:200, Hybridoma Bank), anti-P0 (1:500, Pzo Aves Laboratories) or anti-c-Kit (AF1356, 1:200, R&D Systems) antibodies overnight at 4°C. Secondary antibodies conjugated with Alexa Fluor 488, Alexa Fluor 594, or Alexa Fluor 633 (1:500; Molecular Probes) were applied for 1 hour at 4°C. Nuclei were stained with TO-PRO-3 or 4′,6-diamidino-2-phenylindole (Molecular Probes) in mounting medium. Slides were observed on a confocal laser-scanning microscope (LSM510, Carl Zeiss) equipped with a Ti-Sapphire 2-photon femtosecond laser (MaiTai, Spectra-Physics) using appropriate emission filters. The EGFP signal was confirmed by emission fingerprinting using the LSM 510 META-spectrometer (Carl Zeiss). At least 100 sections for each heart were immunostained, and the results were evaluated by 3 independent observers. For the quantitative analysis of cardiomyocytes, each area was examined in at least 10 sections (80 μm), to avoid duplication in the counting.

Time-Lapse Imaging

Short-axis heart slices (200 μm thick) from the neonatal heart were placed on a Millicell-CM (pore size, 0.4 μm, Millipore, Bedford, MA), mounted in collagen gel, and cultured in Neurobasal medium containing B27 (Invitrogen, San Diego, CA). The dishes were then mounted in a CO_2 incubator chamber (5% CO_2 at 37°C) fitted onto a FV300 confocal microscope (Olympus Optical, Tokyo, Japan). The interventricular septum, left ventricular free wall, and right ventricular region of the neonatal heart were analyzed. Approximately 10 to 20 optical Z sections were obtained automatically every 30 minutes, and ~20 focal planes (~50 μm thickness) were merged to visualize the shape of the entire cell.

Cell Migration Assay

Cell migration assays were conducted in 24-well, 6.5-mm internal-diameter Transwell cluster plates (Corning Costar) on cells prepared from the ventricles of 1-day-old neonatal mice by enzymatic dissociation. After the cells were fully suspended, the EGFP-positive cells were sorted by flow cytometry as described, and 1.0×10^4/100 μL were loaded onto polycarbonate membranes (8-μm pore size) separating the 2 Transwell chambers. B27/0.1% fetal bovine serum (500 μL) containing recombinant human CCL2/MCP-1 (R&D Systems) was added to the lower chambers, and rabbit polyclonal anti-MCP-1 antibodies (100 ng/mL, Abcam) were used to neutralize the MCP-1. Predesigned mouse CCR2 small interfering (si) RNA (MSS203051; Invitrogen) was transfected with Lipofectamine 2000 (Invitrogen) according to the manufacturer's instructions. Briefly, 6 μL of Lipofectamine 2000 was diluted in 1 mL of Opti-MEM I Reduced Serum Medium (Invitrogen), incubated for 15 minutes at room temperature, and mixed with an appropriate amount of CCR2 siRNA (final concentration, 50 nmol/L). After 15 minutes of incubation at room temperature, the mixture was added to each well of sorted NCs. After 24 hours, cells migrating into the lower chamber were counted.

Cell Proliferation Assay

Immediately after MI, mice were injected intraperitoneally with 5-bromo-2′-deoxyuridine (BrdU) (BrdU labeling kit 1296 736, Roche, Basel, Switzerland). Mice were killed 7days after MI and fresh frozen sections were prepared. After antigen retrieval with histoVT One (L6F9587; Nacalai Tesque, Kyoto, Japan) and blocking, BrdU staining was performed according to the manufacturer's instructions.

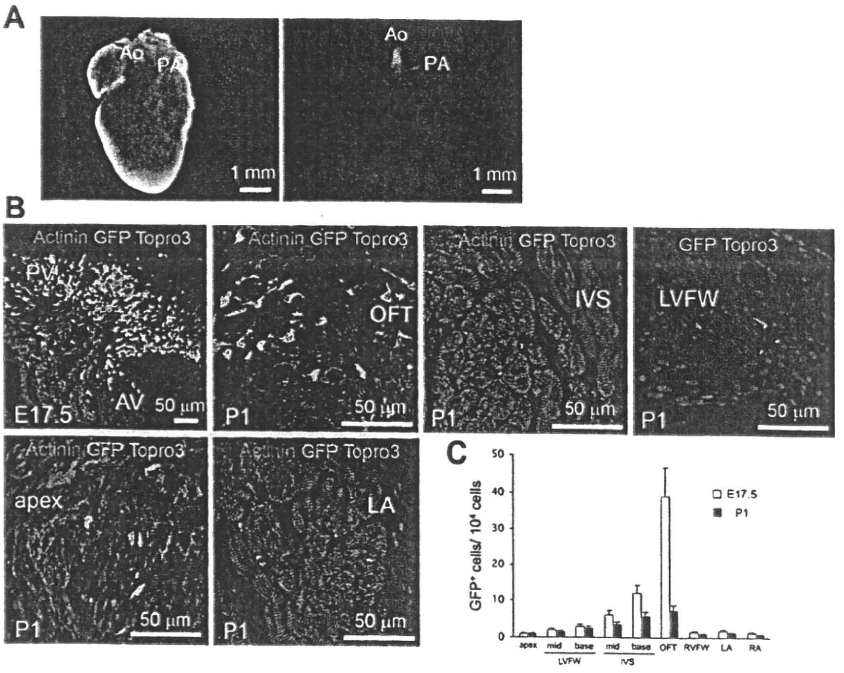

Figure 1. Distribution and characterization of NCSCs in the heart. A, Fluorescence microscope image of the P0-Cre/Floxed-EGFP double-Tg mice heart. Note that the aorta (Ao) and pulmonary artery (PA) are EGFP positive. B, Triple-immunofluorescent staining of the heart. NC cells express the EGFP signal. AV indicates aortic valve; PV, pulmonary valve; OFT, outflow tract; IVS, interventricular septum; LVFW, left ventricular free wall; RVFW, right ventricular free wall; LA, left atrium; RA, right atrium. TO-PRO-3 was used for nuclear staining. C, Distribution of NC cells in the heart. E17.5 indicates embryonic day 17.5.

Reverse Transcription–Polymerase Chain Reaction Analysis

Isolation of RNA and reverse transcription–polymerase chain reaction were performed as described previously.[11] MCP-1 and CCR2 were detected using 0.01 μg of total RNA and the following primers: MCP-1, 5′-GGATCAGAGATACTCATGAT-3′ (forward) and 5′-GAGAAGATTACCTGAGTACA-3′ (reverse); CCR2, 5′-GAGGTCTCGGTTGGGTTGTA-3′ (forward) and 5′-CCACATAGGGATCATGACCC-3′ (reverse).

Statistical Analyses

The values are presented as mean±SEM. Statistical significance was evaluated using unpaired Student *t* tests for comparisons of 2 mean values. Multiple comparisons among 3 or more groups were performed using ANOVA. A value of $P<0.05$ was considered significant.

Results

NC Cells Migrate to and Survive in the Heart

To trace the fate of NC cells, we generated P0-Cre/Floxed-EGFP double-Tg mice (Supplemental Figure I, available online at http://atvb.ahajournals.org). Our initial screening revealed that EGFP-positive cells in these mice were consistent with known NC populations, including those found in the peripheral nervous system, adrenal glands, epidermis, and sympathetic nerve ganglion (Supplemental Figure II).

At postnatal day 1, EGFP fluorescence was observed in the aorta, pulmonary artery, and outflow tract of the heart in each P0-Cre/Floxed-EGFP mouse (Figure 1A). On postnatal day 1 and embryonic day 17.5, immunohistological analyses revealed EGFP-positive cells densely distributed at the septum between the aorta and pulmonary artery, as well as in the outflow tract (Figure 1B). Notably, nucleated EGFP-positive cells were detected in the interventricular septum, left ventricular free wall, apex, and both atria (Figure 1C); these EGFP-positive cells were small and immunonegative for actinin.

The Dynamic Movement of NCSCs in Murine Heart

We next attempted to isolate EGFP-positive cells from the neonatal hearts by fluorescence-activated cell sorting. Using pseudo-2-dimensional separation with 2 band-pass filters for green fluorescent protein and allophycocyanin, the EGFP-positive cells were localized above the diagonal line as a distinct population (population 1) (Figure 2A). Among the total cells in a whole heart dissected from 1-day-old P0-Cre/Floxed-EGFP mice, 0.2±0.02% cells were EGFP positive. These cells were then sorted again using specific antibodies against nestin, c-kit, and sca-1 (Figure 2B), resulting in 37.5±1.5% nestin/EGFP-positive cells, 2.2±0.4% c-kit/EGFP-positive cells, and no sca-1/EGFP-positive cells. The existence of cells positive for both nestin and EGFP was confirmed by immunohistological analyses (Figure 2C). The outflow tract of 1-day-old P0-Cre/Floxed-EGFP mice showed most EGFP-positive cells expressing nestin. None of these double-positive cells expressed actinin. Furthermore, we performed a sphere-forming assay, in which EGFP-positive cells were collected from the ventricles of 1-day-old P0-Cre/Floxed-EGFP mice by flow cytometry and cultured at a clonal density of 5×10^3 cells/mL in serum-free sphere-forming medium that contained human epidermal growth factor, human fibroblast growth factor 2, and B27. The EGFP-positive cells proliferated to form spheres that were morphologically similar to neurospheres after 14 days (Supplemental Figure III). These spheres expressed nestin and P75 nerve growth factor receptor ($p75^{NGFR}$) but did not express either c-kit or sca-1.

Next, we sought to visualize any NCSC migration in the myocardium in vivo. Time-lapse video imaging of slice cultures from postnatal P0-Cre/Floxed-EGFP mice revealed that the EGFP-positive NCSCs were indeed dynamic (Figure 2D and Supplemental Video). The migration rate of these EGFP-

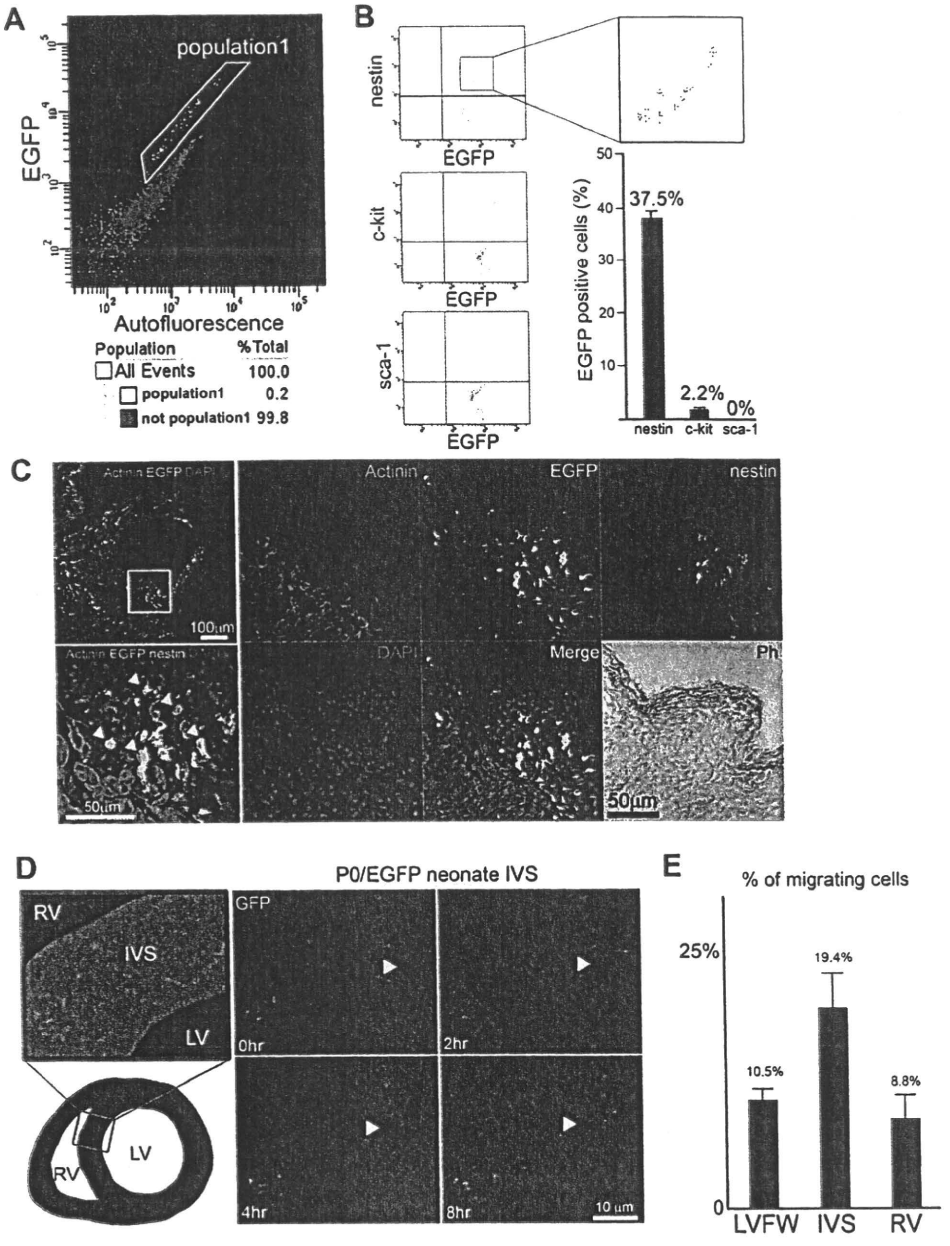

Figure 2. Number of NCSCs in the heart and the ratios of stem cell markers. A, The EGFP-positive cells were separated as a distinct population (population 1) from the non-stained cells with autofluorescence using 2 band-pass filters for green fluorescent protein and allophycocyanin. A representative 2-dimensional separation is shown. B, The EGFP-positive cells were secondarily sorted using antibodies against nestin, c-kit, and sca-1. Representative 2-dimensional separation is shown. Numbers of cells positive for nestin as a proportion of the EGFP-expressing cells are summarized in the bar graph (n=3). C, Quadruple immunofluorescence of heart from a 1-day-old P0-Cre/Floxed-EGFP mouse. Ph indicates phase-contrast image; DAPI, 4′,6-diamidino-2-phenylindole. D, Tracing of cell movement. The time-lapse images obtained from slice culture samples (200 μm thickness) of neonatal P0-Cre/Floxed–EGFP mouse. Representative images from interventricular septum are shown. Schematic drawing shows the positional tracing of the cell movement. RV indicates right ventricle; IVS, interventricular septum; LV, left ventricle. Note that some EGFP-expressing cells are moving (arrows). E, Quantification of migrating cells in left ventricular free wall (LVFW), interventricular septum (IVS), and right ventriculum (RV) (n=5).

positive NCSCs was higher in the interventricular septum than that in the left or right ventricular free wall (Figure 2E).

NCSCs Spontaneously Differentiate Into Cardiomyocytes in Postnatal Heart

We next investigated whether the EGFP-positive NC cells could differentiate into cardiomyocytes in vivo under physiological conditions. EGFP-positive cardiomyocytes were not detected during the neonatal stage or in the first week after birth but appeared at 2 weeks postnatally and increased in number thereafter (Figure 3A). At 10 weeks of age, the EGFP-positive cardiomyocytes were detected throughout the heart, being most abundant at the basal interventricular septum (Figure 3B and 3C). Although there was a corresponding decrease in the number of actinin-negative nucleated EGFP-positive cells as the heart grew, these cells persisted in the adult heart (Figure 3D), where they tended to form clusters and expressed connexin 43 (Figure 3E) and GATA4 (Figure 3F).

To confirm whether NCSCs contribute to the provision of cardiomyocytes during postneonatal maturation, we examined the hearts from 2 different Tg murine models with genetically tagged NC cells. NCSC-derived cardiomyocytes (actinin-positive, EGFP-positive cells) were observed in the left ventricles of both plasminogen activator–Cre[18]/Floxed EGFP mice (Figure 3G) and Wnt-1[19]-Cre/floxed-EGFP mice (Figure 3H).

NC Cells Accumulate in the BZA After MI

We also investigated the pathophysiological role of cardiac NC cells by inducing MI and observing the contribution of these cells to the repair process. Many EGFP-positive cells were observed in the ischemic BZA and infarct area (Figure 4A), with 10-fold more EGFP-positive cells in the BZA than

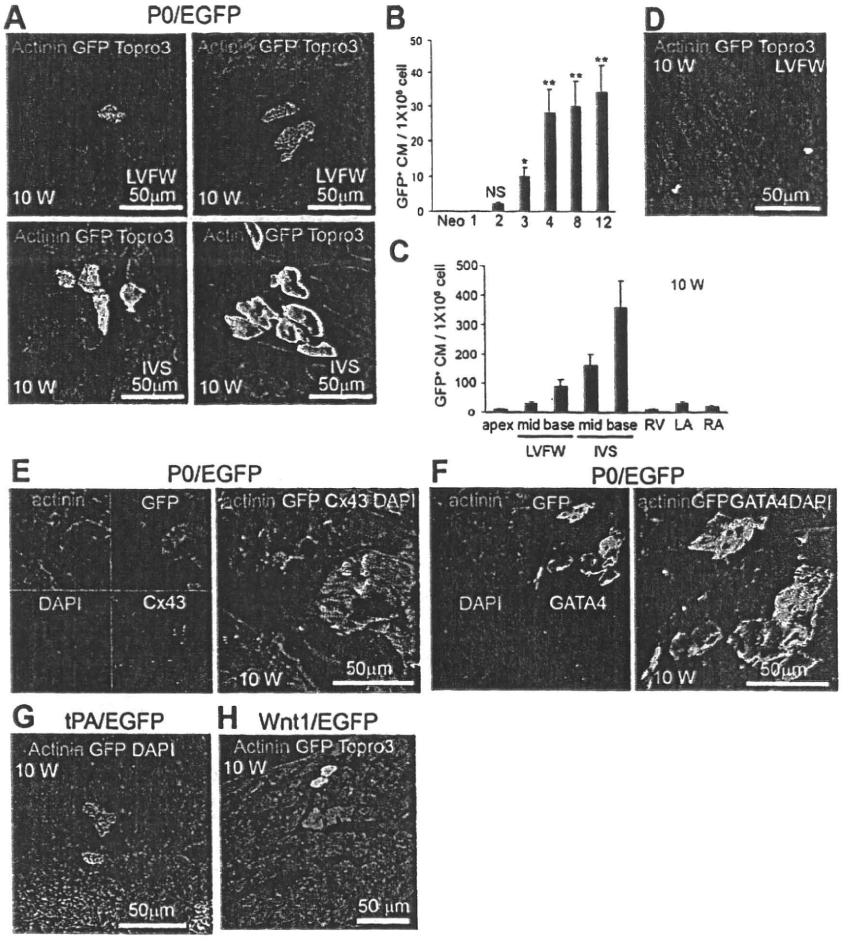

Figure 3. NCSC-derived cardiomyocytes emerge and increase in number during postneonatal growth. A, Immunofluorescence of NCSC-derived cardiomyocytes from 10-week (W)–old P0-Cre/Floxed-EGFP mice. IVS indicates interventricular septum; LVFW, left ventricular free wall; GFP, green fluorescent protein. B, Kinetics of EGFP-positive cardiomyocyte appearance (*P<0.01; **P<0.001; NS indicates not significant compared with the number observed on neonatal day 1). C, Distribution of EGFP-positive cardiomyocytes. D, EGFP-positive nonmyocytes in 10-week-old P0-Cre/Floxed-EGFP mice. E, Immunostaining of EGFP-positive cardiomyocytes with anti-connexin 43 antibody (Cx43, red) and 4′,6-diamidino-2-phenylindole (DAPI). F, Immunostaining of EGFP-positive cardiomyocytes with anti-GATA4 antibody and DAPI. G and H, Immunostaining of EGFP-positive cardiomyocytes in plasminogen activator (tPA)–Cre/Floxed EGFP mice and Wnt-1-Cre/Floxed EGFP mice.

in the nonischemic area (Figure 4B). Emission spectrum measurements confirmed that the green fluorescence was produced by EGFP and were not due to autofluorescence from inflammatory cells (Figure 4A, right). The BrdU incorporation study revealed that most EGFP-positive cells in the BZA were proliferating (Supplemental Figure IV). However, BrdU incorporation was barely detectable in nestin-positive cells. The EGFP-positive cell numbers in the BZA were increased by 1 week post-MI, peaked at 1 month post-MI, and then decreased gradually thereafter (Figure 4C). These cells were particularly concentrated in the vicinity of the surviving cardiomyocytes facing the necrotic area (Figure 4D). Some nucleated EGFP-expressing cells were also nestin-positive (Figure 4E). These cells were negative for c-Kit. The c-Kit-positive cells tended to be in different clusters and were negative for EGFP (Figure 4F).

MCP-1 Induces NCSC Migration

The nestin-positive NC cells accumulated in the BZA and infarct area after MI. We then asked how the EGFP-positive NCSCs could migrate toward these foci of active myocardial injury after MI. MCP-1 expression was also detected at 1 week post-MI in the ischemic BZA, peaking at 2 weeks post-MI, and decreasing thereafter (Figure 5A). In addition, the MCP-1 receptor CCR2 was constitutively expressed on the surface of NCSCs, although at lower levels than on bone marrow cells (Figure 5B).To examine whether this MCP-1 expression in the BZA could drive the NCSC migration via interactions with CCR2, NCSCs were isolated from postnatal hearts and subjected to cell migration assay (Figure 5C). MCP-1 at the lowest dose of 0.1 ng/mL induced NCSC migration in vitro, with the maximum migration rate reached at 1.0 ng/mL MCP-1. This cell migration was completely abolished in the presence of neutralizing antibodies against MCP-1 or by the addition of CCR2 siRNA into the media bathing the sorted cells (Figure 5D and 5E). These results suggested that MCP-1 provides important guidance cues for NCSC migration after MI.

NCSCs From Adult Heart Contribute to Regeneration After MI

We finally investigated whether NCSCs could differentiate into cardiomyocytes after MI. EGFP-positive cardiomyocytes were observed in the BZA of P0-Cre/Floxed-EGFP mice (Figure 6A), adjacent to both the surviving cardiomyocytes and the infarcted area, and no EGFP-positive cardiomyocytes were observed at the center of the infarcted area. These EGFP-positive cells were smaller than the surrounding cardiomyocytes (Figure 6B). The EGFP-positive cardiomyocytes first appeared at 2 weeks post-MI, and gradually increased in number to peak at 4 weeks post-MI (Figure 6C).

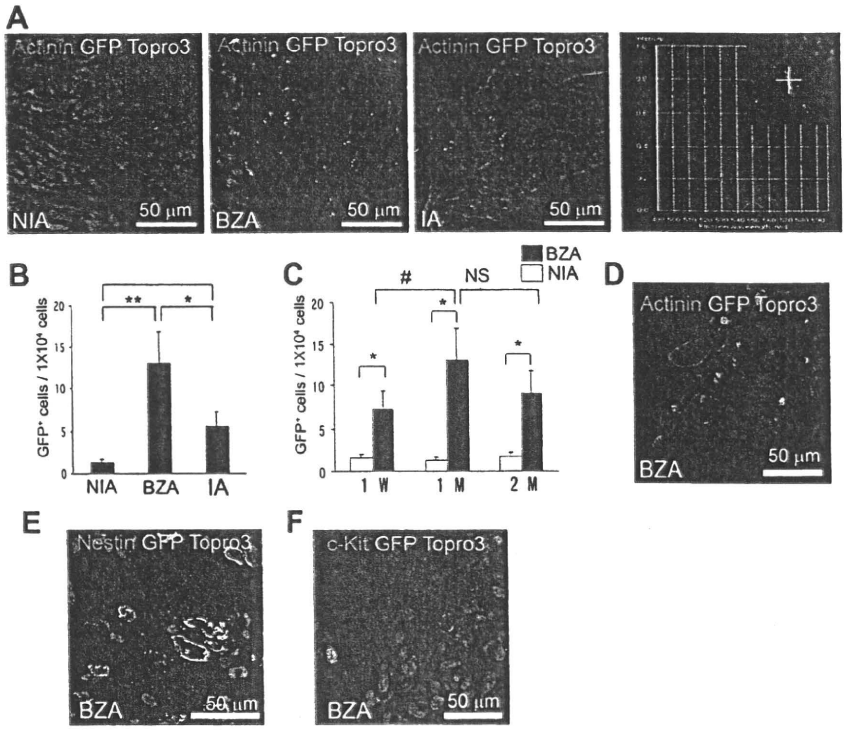

Figure 4. NCSCs accumulate at the ischemic border zone after MI. A, Immunostaining of the nonischemic area (NIA), BZA, and infarct area (IA) with anti-actinin antibody (red) and TO-PRO-3. The right panel shows the emission spectrum values for the EGFP-positive cells. B, Quantitative analysis of EGFP-positive cells in the NIA, BZA, and IA (**P<0.001, NIA vs BZA; *P<0.01, BZA vs IA; #P<0.05, NIA vs IA). C, Kinetics of EGFP-positive cell appearance in the BZA and NIA (*P<0.01, NIA vs BZA; #P<0.05, 1 week vs 1 month; NS indicates not significant, 1 month vs 2 months). GFP, green fluorescent protein. D, Immunostaining of EGFP-positive cells in the BZA. Note that the EGFP-positive cells are concentrated in the vicinity of the surviving cardiomyocytes. E, Immunostaining of EGFP-positive cells for nestin (left). Note that the EGFP-positive cells in the BZA are positive for nestin, which suggests that they are NCSCs. F, c-Kit-positive small cardiomyocytes also emerged as a distinct cluster.

Discussion

During embryogenesis, NC cells migrate into tissues and differentiate into various cell types, although some persist as NCSCs in the adult. Using genetically tagged cells arising from neural crest, we demonstrated that NC cells migrated into the developing heart. Flow cytometric analysis of cells isolated from the whole heart of 1-day-old mice revealed that 0.2±0.02% of total cells were NC cells. Of these, 37.5±1.5% expressed nestin, a marker of undifferentiated neuronal precursor cells, indicating that they are retained in the hearts as dormant NCSCs. NCSCs were localized predominantly in the outflow tract, but they were also distributed throughout ventricular myocardium in a decreasing gradient from base to apex. Notably, we successfully visualized the dynamic nature of NC cells in the ventricular wall by time-lapse imaging of living myocardial slice cultures. The number of NCSCs decreased as the heart grew, but some cells persisted in the adult heart. Interestingly, these cells were strikingly accumulated in the ischemic border zone after MI and contributed to the regeneration of injured myocardium, at least in part, via differentiation into cardiomyocytes. Ex vivo migration assays further suggested that MCP-1 secreted from the BZA acts as an important guidance molecule for NC cell migration.

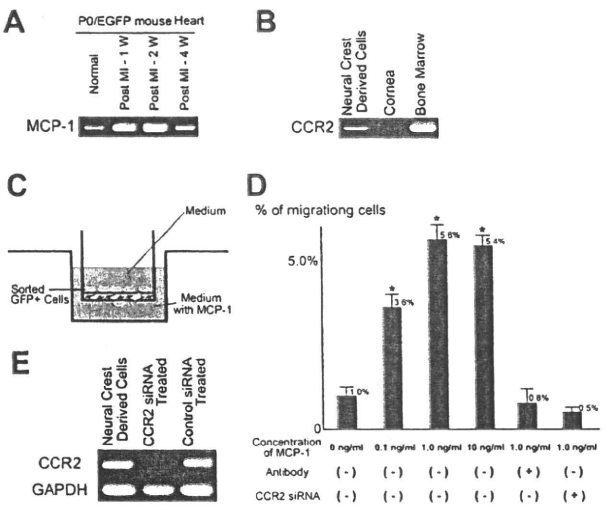

Figure 5. Chemotactic effect of MCP-1 on NCSC migration. (A) Expression of MCP-1 in the heart by reverse transcription–polymerase chain reaction analysis. Samples represent normal control heart (not infarcted) and ischemic BZA at 1, 2, and 4 weeks (W) after MI. B, The expression of CCR-2 in NCSCs by reverse transcription–polymerase chain reaction analysis. Cornea and bone marrow are used as negative control and positive control samples respectively. C, Schematic representation of cell migration assay. GFP indicates green fluorescent protein. D, Quantitative analyses of the chemotactic effect of MCP-1 on NCSC migration. MCP-1 antibodies or CCR2 siRNA reduced the migration of NCSC (n=10; *P<0.05 compared with MCP-1-free conditions). E, Reverse transcription–polymerase chain reaction analysis of CCR2 expression in NC cells.

In the present study, we used P0 to trace the fate of the neural crest cell lineage. In the P0-Cre/Floxed EGFP mice, we confirmed that the EGFP-expressing cells were consistent with known NC populations. As a negative control, we examined the immunofluorescence patterns in P0-Cre and floxed-EGFP single-Tg mice and detected no EGFP-positive cells. We also ruled out autofluorescence from irrelevant cells. We do not believe that the appearance of EGFP-positive cells in the hearts of P0-Cre/Floxed EGFP mice simply reflects unanticipated induction of P0 expression in the postnatal mesoderm-derived cardiomyocytes, as EGFP-positive cardiomyocytes were also observed in hearts from other Tg mice models that can trace the fate of NC-cells, such as tissue plasminogen activator–Cre[18]/Floxed EGFP mice and Wnt-1-Cre[19]/floxed-EGFP mice.

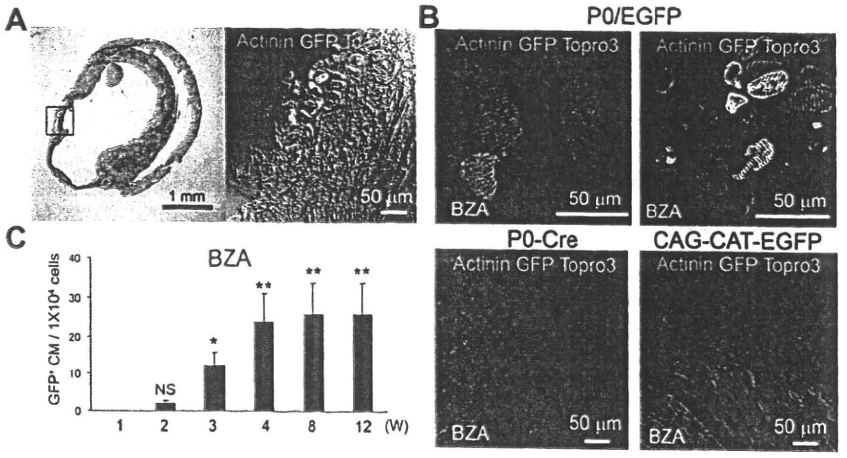

Figure 6. NCSCs contribute to the regeneration of cardiomyocytes after MI. A, Azan staining of an infarcted heart and serial sections immunostained for actinin. Right panel shows a high-magnification image of the inset in the left panel. B, Immunostaining for actinin in the BZAs of P0-Cre/Floxed-EGFP mice and their littermates (P0-Cre and CAG-CAT$^{loxP/loxP}$-EGFP mice) at 8 weeks (W) post-MI. Note the relatively small EGFP-positive cardiomyocytes appearing at the BZA. C, Kinetics of EGFP-positive cardiomyocyte appearance in the nonischemic area, BZA, and IA after MI (*$P<0.01$, **$P<0.001$ compared with 1 week post-MI).

The nestin-positive NC cells accumulated in the BZA and infarct area after MI. This phenomenon resembles the behavior of neural stem cells in brain, where they remain in the subventricular zone as dormant stem cells.[21] On differentiation into neuroblasts, these neural stem cells migrate to the olfactory bulb under normal physiological conditions,[22] whereas they migrate and differentiate into mature neurons in the poststroke adult striatum[23] under the influence of chemokines (chemotactic cytokines) secreted from the infarct area.[24]

We previously demonstrated primitive NC cells migrating from the cardiac neural crest during embryonic development and remaining in the heart as dormant stem cells.[11] Although NCSCs were localized predominantly in the outflow tract, they were also distributed throughout ventricular myocardium and were obviously dynamic. On the basis of these similarities, we propose that the migration of cardiac NCSCs in the BZA is induced by paracrine factors from the infarct area.

Chemokines are small heparin-binding proteins whose main function is to regulate cell trafficking. Once induced, the direct migration of cells expressing the appropriate chemokine receptors occurs along a chemical ligand gradient, whereby cells move more strongly toward the higher concentration of chemokines.[25] MCP-1 is a key chemokine in the regulation of migration and infiltration of monocyte/macrophages.[26] MCP-1 expression and function has also been implicated in the pathogenesis of cardiovascular diseases.[27] MCP-1 causes diapedesis of monocytes from the lumen to the subendothelial space, where they become foam cells, initiating fatty streak formation that leads to atherosclerotic plaque formation. Studies in Tg mice expressing MCP-1, the knockout MCP-1 gene, or the MCP-1 receptor CCR2 indicated that the MCP-1/CCR2 system functions in recruiting monocytes to atheroma.[28–32] The pathogenesis of restenosis after balloon angioplasty involves the migration of medial smooth muscle cells across the internal elastic lamina to form a neointima. Accumulating evidence indicated that balloon injury induces local MCP-1 production and anti-MCP-1/CCR2 approaches could cause significant reduction in neointimal hyperplasia.[33–35] MCP-1 also has a critical role in the early recruitment of macrophages to the healing infarct. MCP-1-deficient animals exhibit reduced and delayed infiltration of mononuclear cells into infarcted heart, resulting in impaired replacement of injured cardiomyocytes with granulation tissues, impaired macrophage differentiation, and diminished myofibroblast infiltration.[36]

In the present study, we demonstrated a novel function of MCP-1 via its chemotactic activity. The MCP-1 receptor CCR2 is constitutively expressed on the surface of NCSCs, and ex vivo cell migration assays demonstrated that MCP-1 induces NCSC migration in a dose-dependent manner that was completely abolished by neutralizating antibodies against MCP-1. These results suggested that direct migration of NCSCs expressing CCR2 occurs along an chemotactic MCP-1 gradient. However, the production of MCP-1 could in turn elicit blood cell migration into the heart. Thus, EGFP-positive NCSCs from bone marrow should also be considered as an alternative source of EGFP-positive cardiomyocytes.[37] Future studies are necessary to clarify the quantitative contribution between cardiac-resident and bone marrow-derived NCSCs in terms of myocardial regeneration after MI.

NCSCs have a capacity for self-renewal, migration, and differentiation. The factors supporting NCSC self-renewal and differentiation have been described previously: the synergistic activity of Wnt and brain natriuretic peptide signaling regulates NCSC self-renewal, whereas each individual factor alone promotes lineage decision.[38] The transforming growth factor-β family promotes autonomic neurogenesis and the development of smooth muscle-like cells, whereas neuregulin-1 induces the generation of peripheral glia. In the present study, we found that MCP-1/CCR2 signaling plays a key role in NCSC migration following the ischemic insult. Whether MCP-1/CCR2 signaling also stimulates NCSC self-renewal remains unknown. In the ischemic border zone, BrdU incorporation into the NCSCs was barely detectable. Most of the BrdU-positive NC-derived cells are lineage-committed cells. Thus, we do not think that MCP-1/CCR2 signaling stimulates NCSC self-renewal.

In conclusion, cardiac NCSCs represent a source of cardiomyocytes for postneonatal heart growth and cardiac regeneration after MI. NCSCs may have clinical importance and should be studied further, because cardiosphere culturing is a feasible method for the isolation of cardiac stem cells from human heart biopsies.

Sources of Funding

This study was supported by the Program for Promotion of Fundamental Studies in Health Science of the National Institute of

Biomedical Innovation, Japan, and by research grants from the Ministry of Education, Science and Culture, Japan.

Disclosures

None.

References

1. Beltrami AP, Barlucchi L, Torella D, Baker M, Limana F, Chimenti S, Kasahara H, Rota M, Musso E, Urbanek K, Leri A, Kajstura J, Nadal-Ginard B, Anversa P. Adult cardiac stem cells are multipotent and support myocardial regeneration. *Cell*. 2003;114:763–776.
2. Oh H, Bradfute SB, Gallardo TD, Nakamura T, Gaussin V, Mishina Y, Pocius J, Michael LH, Behringer RR, Garry DJ, Entman ML, Schneider MD. Cardiac progenitor cells from adult myocardium: homing, differentiation, and fusion after infarction. *Proc Natl Acad Sci U S A*. 2003;100: 12313–12318.
3. Hierlihy AM, Seale P, Lobe CG, Rudnicki MA, Megeney LA. The post-natal heart contains a myocardial stem cell population. *FEBS Lett*. 2002;530:239–243.
4. Cai CL, Liang X, Shi Y, Chu PH, Pfaff SL, Chen J, Evans S. Isl1 identifies a cardiac progenitor population that proliferates prior to differentiation and contributes a majority of cells to the heart. *Dev Cell*. 2003;5:877–889.
5. Douarin LM, Kalcheim C. *The Neural Crest*. Cambridge, UK: Cambridge University Press; 1999.
6. Gammill LS, Bronner-Fraser M. Neural crest specification: migrating into genomics. *Nat Rev Neurosci*. 2003;4:795–805.
7. Hall BK. The neural crest as a fourth germ layer and vertebrates as quadroblastic not triploblastic. *Evol Dev*. 2000;2:3–5.
8. Toma JG, Akhavan M, Fernandes KJ, Barnabe-Heider F, Sadikot A, Kaplan DR, Miller FD. Isolation of multipotent adult stem cells from the dermis of mammalian skin. *Nat Cell Biol*. 2001;3:778–784.
9. Fernandes KJ, McKenzie IA, Mill P, Smith KM, Akhavan M, Barnabe-Heider F, Biernaskie J, Junek A, Kobayashi NR, Toma JG, Kaplan DR, Labosky PA, Rafuse V, Hui CC, Miller FD. A dermal niche for multipotent adult skin-derived precursor cells. *Nat Cell Biol*. 2004;6: 1082–1093.
10. Yoshida S, Shimmura S, Nagoshi N, Fukuda K, Matsuzaki Y, Okano H, Tsubota K. Isolation of multipotent neural crest-derived stem cells from the adult mouse cornea. *Stem Cells*. 2006;24:2714–2722.
11. Tomita Y, Matsumura K, Wakamatsu Y, Matsuzaki Y, Shibuya I, Kawaguchi H, Ieda M, Kanakubo S, Shimazaki T, Ogawa S, Osumi N, Okano H, Fukuda K. Cardiac neural crest cells contribute to the dormant multipotent stem cell in the mammalian heart. *J Cell Biol*. 2005;170: 1135–1146.
12. Kaneko Y, Sakakibara S, Imai T, Suzuki A, Nakamura Y, Sawamoto K, Ogawa Y, Toyama Y, Miyata T, Okano H. Musashi1: an evolutionally conserved marker for CNS progenitor cells including neural stem cells. *Dev Neurosci*. 2000;22:139–153.
13. Yamauchi Y, Abe K, Mantani A, Hitoshi Y, Suzuki M, Osuzu F, Kuratani S, Yamamura K. A novel transgenic technique that allows specific marking of the neural crest cell lineage in mice. *Dev Biol*. 1999;212: 191–203.
14. Kawamoto S, Niwa H, Tashiro F, Sano S, Kondoh G, Takeda J, Tabayashi K, Miyazaki J. A novel reporter mouse strain that expresses enhanced green fluorescent protein upon cre-mediated recombination. *FEBS Lett*. 2000;470:263–268.
15. Lemke G, Lamar E, Patterson J. Isolation and analysis of the gene encoding peripheral myelin protein zero. *Neuron*. 1988;1:73–83.
16. Bhattacharyya A, Frank E, Ratner N, Brackenbury R. P0 is an early marker of the Schwann cell lineage in chickens. *Neuron*. 1991;7: 831–844.
17. Nagoshi N, Shibata S, Kubota Y, Nakamura M, Nagai Y, Satoh E, Morikawa S, Okada Y, Mabuchi Y, Katoh H, Okada S, Fukuda K, Suda T, Matsuzaki Y, Toyama Y, Okano H. Ontogeny and multipotency of neural crest-derived stem cells in mouse bone marrow, dorsal root ganglia, and whisker pad. *Cell Stem Cell*. 2008;2:392–403.
18. Pietri T, Eder O, Blanche M, Thiery JP, Dufour S. The human tissue plasminogen activator-Cre mouse: a new tool for targeting specifically neural crest cells and their derivatives in vivo. *Dev Biol*. 2003;259: 176–187.
19. Danielian PS, Muccino D, Rowitch DH, Michael SK, McMahon AP. Modification of gene activity in mouse embryos in utero by a tamoxifen-inducible form of Cre recombinase. *Curr Biol*. 1998;8:1323–1326.
20. Kawada H, Fujita J, Kinjo K, Matsuzaki Y, Tsuma M, Miyatake H, Muguruma Y, Tsuboi K, Itabashi Y, Ikeda Y, Ogawa S, Okano H, Hotta T, Ando K, Fukuda K. Nonhematopoietic mesenchymal stem cells can be mobilized and differentiate into cardiomyocytes after myocardial infarction. *Blood*. 2004;104:3581–3587.
21. Gage FH. Mammalian neural stem cells. *Science*. 2000;287:1433–1438.
22. Sawamoto K, Wichterle H, Gonzalez-Perez O, Cholfin JA, Yamada M, Spassky N, Murcia NS, Garcia-Verdugo JM, Marin O, Rubenstein JL, Tessier-Lavigne M, Okano H, Alvarez-Buylla A. New neurons follow the flow of cerebrospinal fluid in the adult brain. *Science*. 2006;311: 629–632.
23. Arvidsson A, Collin T, Kirik D, Kokaia Z, Lindvall O. Neuronal replacement from endogenous precursors in the adult brain after stroke. *Nat Med*. 2002;8:963–970.
24. Yamashita T, Ninomiya M, Hernandez Acosta P, Garcia-Verdugo JM, Sunabori T, Sakaguchi M, Adachi K, Kojima T, Hirota Y, Kawase T, Araki N, Abe K, Okano H, Sawamoto K. Subventricular zone-derived neuroblasts migrate and differentiate into mature neurons in the post-stroke adult striatum. *J Neurosci*. 2006;26:6627–6636.
25. Callewaere C, Banisadr G, Rostene W, Parsadaniantz SM. Chemokines and chemokine receptors in the brain: implication in neuroendocrine regulation. *J Mol Endocrinol*. 2007;38:355–363.
26. Gu L, Okada Y, Clinton SK, Gerard C, Sukhova GK, Libby P, Rollins BJ. Absence of monocyte chemoattractant protein-1 reduces atherosclerosis in low density lipoprotein receptor-deficient mice. *Mol Cell*. 1998;2: 275–281.
27. Niu J, Kolattukudy PE. Role of MCP-1 in cardiovascular disease: molecular mechanisms and clinical implications. *Clin Sci (Lond)*. 2009; 117:95–109.
28. Aiello RJ, Bourassa PA, Lindsey S, Weng W, Natoli E, Rollins BJ, Milos PM. Monocyte chemoattractant protein-1 accelerates atherosclerosis in apolipoprotein E-deficient mice. *Arterioscler Thromb Vasc Biol*. 1999; 19:1518–1525.
29. Gu L, Tseng SC, Rollins BJ. Monocyte chemoattractant protein-1. *Chem Immunol*. 1999;72:7–29.
30. Zhong L, Chen WQ, Ji XP, Zhang M, Zhao YX, Yao GH, Zhang PF, Zhang C, Zhang Y. Dominant-negative mutation of monocyte chemoattractant protein-1 prevents vulnerable plaques from rupture in rabbits independent of serum lipid levels. *J Cell Mol Med*. 2008;12:2362–2371.
31. Gosling J, Slaymaker S, Gu L, Tseng S, Zlot CH, Young SG, Rollins BJ, Charo IF. MCP-1 deficiency reduces susceptibility to atherosclerosis in mice that overexpress human apolipoprotein B. *J Clin Invest*. 1999;103: 773–778.
32. Boring L, Gosling J, Cleary M, Charo IF. Decreased lesion formation in CCR2-/- mice reveals a role for chemokines in the initiation of atherosclerosis. *Nature*. 1998;394:894–897.
33. Guzman RJ, Lemarchand P, Crystal RG, Epstein SE, Finkel T. Efficient and selective adenovirus-mediated gene transfer into vascular neointima. *Circulation*. 1993;88:2838–2848.
34. Egashira K, Zhao Q, Kataoka C, Ohtani K, Usui M, Charo IF, Nishida K, Inoue S, Katoh M, Ichiki T, Takeshita A. Importance of monocyte chemoattractant protein-1 pathway in neointimal hyperplasia after periarterial injury in mice and monkeys. *Circ Res*. 2002;90:1167–1172.
35. Horvath C, Welt FG, Nedelman M, Rao P, Rogers C. Targeting ccr2 or cd18 inhibits experimental in-stent restenosis in primates: inhibitory potential depends on type of injury and leukocytes targeted. *Circ Res*. 2002;90:488–494.
36. Dewald O, Zymek P, Winkelmann K, Koerting A, Ren G, Abou-Khamis T, Michael LH, Rollins BJ, Entman ML, Frangogiannis NG. CCL2/ monocyte chemoattractant protein-1 regulates inflammatory responses critical to healing myocardial infarcts. *Circ Res*. 2005;96:881–889.
37. Endo J, Sano M, Fujita J, Hayashida K, Yuasa S, Aoyama N, Takehara Y, Kato O, Makino S, Ogawa S, Fukuda K. Bone marrow derived cells are involved in the pathogenesis of cardiac hypertrophy in response to pressure overload. *Circulation*. 2007;116:1176–1184.
38. Kleber M, Lee HY, Wurdak H, Buchstaller J, Riccomagno MM, Ittner LM, Suter U, Epstein DJ, Sommer L. Neural crest stem cell maintenance by combinatorial Wnt and BMP signaling. *J Cell Biol*. 2005;169: 309–320.

Supplemental figure I

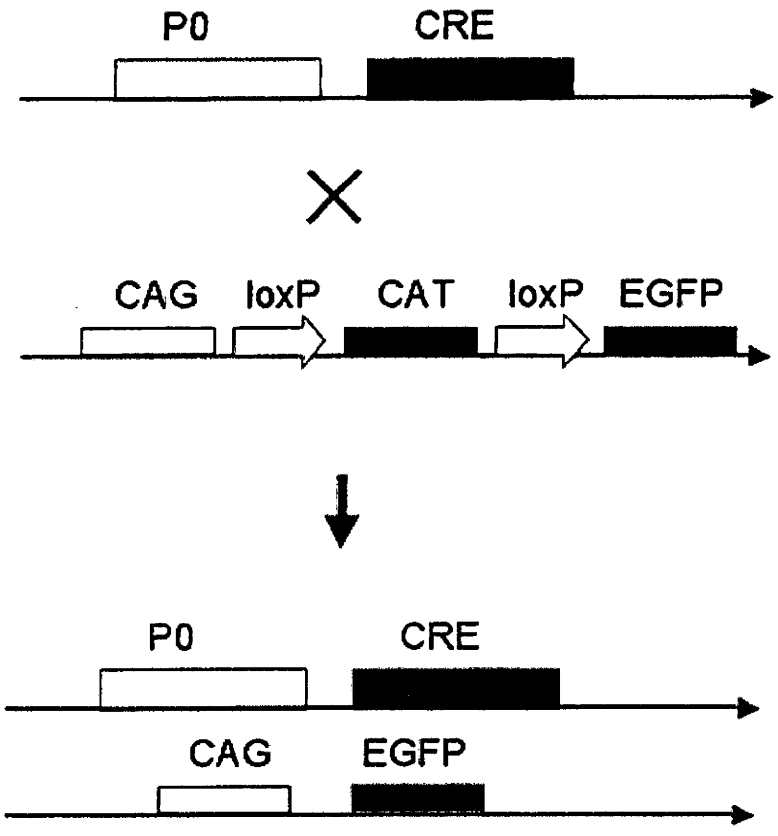

Supplemental figure II

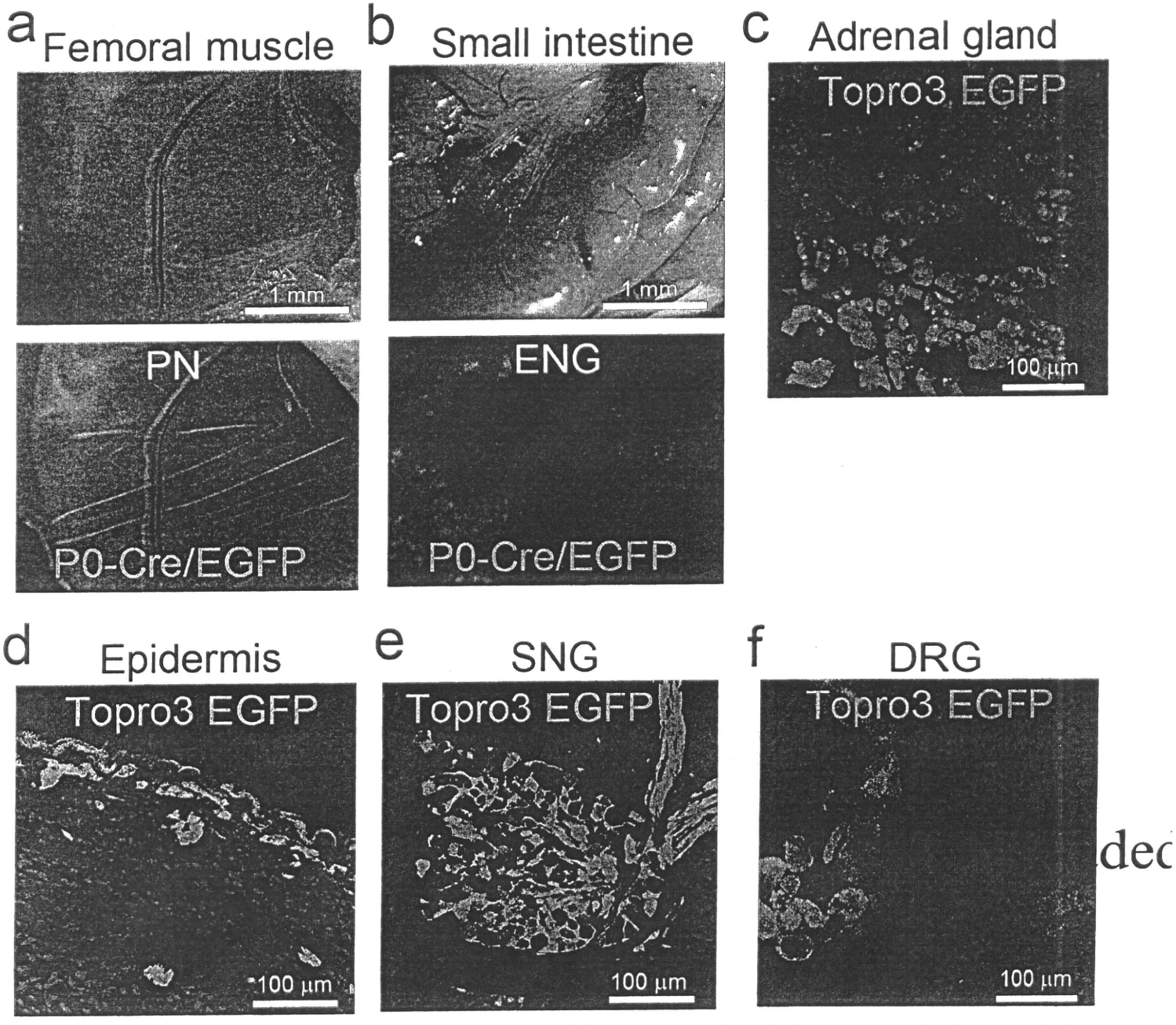

dec

Supplemental figure III

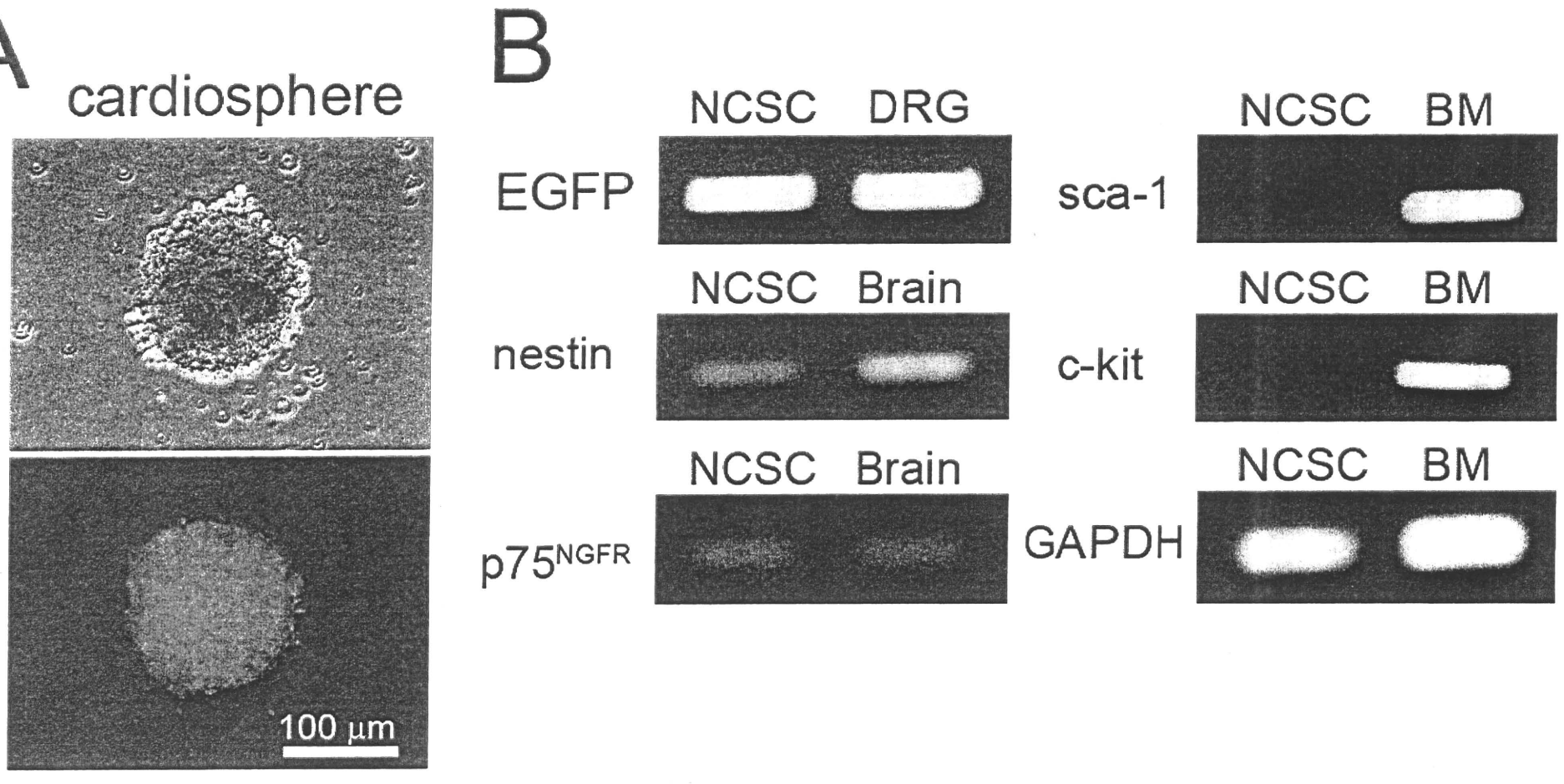

Supplemental figure IV

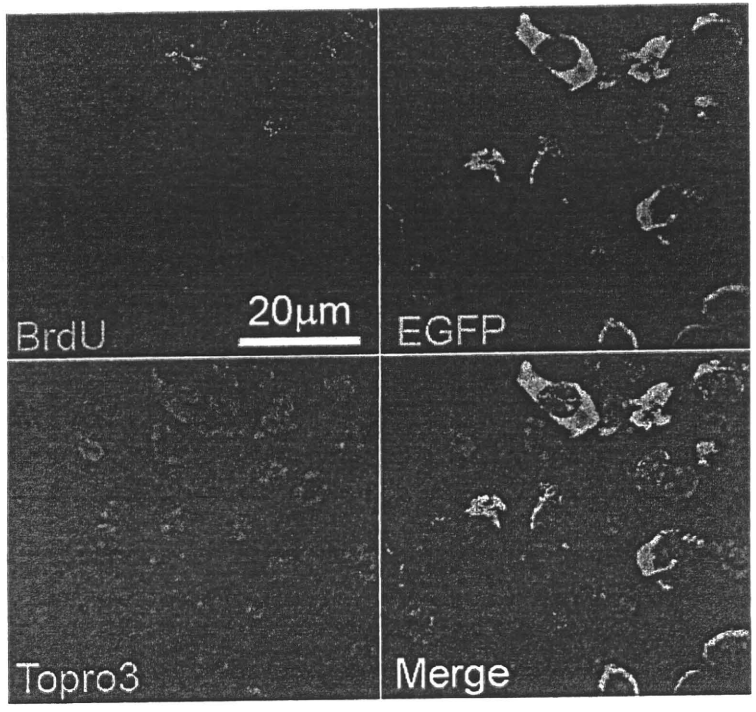

Safety and efficacy of pericardial endoscopy by percutaneous subxyphoid approach in swine heart in vivo

Takehiro Kimura, MD,[a] Shunichiro Miyoshi, MD, PhD,[a] Seiji Takatsuki, MD, PhD,[a] Kojiro Tanimoto, MD, PhD,[a] Kotaro Fukumoto, MD, PhD,[a] Kyoko Soejima, MD, PhD,[b] and Keiichi Fukuda, MD, PhD[a]

Objective: A nonsurgical approach from the epicardial surface is useful for various cardiac interventions, such as positioning of the left ventricular lead for cardiac resynchronization therapy and epicardial ablation. Stem cell delivery on the epicardial surface can be considered in the future if good quality of visualization can be obtained. However, because the pericardial space is limited, hemodynamic conditions may deteriorate with pericardial endoscopy. Therefore, the feasibility and efficacy of pericardial endoscopy were examined by using ready-made endoscopes.

Methods: Anesthetized swines (26–61 kg; n = 6) were used for the experiment. Electrocardiogram, femoral artery blood pressure, and oxygen saturation by pulse oximetry were continuously monitored during the procedures. Guided by the fluoroscopy, sheaths were advanced to the pericardial space using the modified Seldinger technique from the subxyphoid space.

Results: After insertion of an endoscope with a maximum diameter of 6.9 mm, hemodynamic parameters were stable during the procedure with atropine. Stable and acceptable endoscopic images were obtained. Minor operations can be performed with pericardial endoscopic-guided laparoscopic forceps with no complications.

Conclusions: The endoscopic pericardial procedure is effective and feasible. This procedure can increase the possibility and efficacy of nonsurgical treatment for cardiac diseases. (J Thorac Cardiovasc Surg 2010;■:1-10)

ET/BS

Video clip is available online.

Recent progress in minimally invasive therapy has dramatically changed the treatment of heart disease. Percutaneous transluminal approaches (eg, coronary angioplasty[1]; catheter ablation[2,3]; pacemaker, implantable cardioverter defibrillator, and cardiac resynchronization therapy[4]; and percutaneous heart valve replacement[5]) have provided significant therapeutic benefit to patients with a minimal burden. However, it is still difficult to reach the epicardial targets by the transluminal approach. Minimally invasive epicardial approaches may aid epicardial biopsy, implantation of left ventricular epicardial pacing lead for cardiac resynchronization therapy, and ablation for epicardial arrhythmic substrate. Furthermore, such approaches are also applicable for transplantation of stem cells into the myocardium. Although significant progress in research for cardiac stem cells has been made, research for optimization of the transplantation procedures is sparse. Compared with catheter-based transluminal stem cell transplantation,[6] epicardial transplantation poses less risk for infusion of stem cells into the bloodstream and systemic dissemination and microembolization of overflowed stem cells.[7,8] Pericardial endoscopy is also applicable to direct genetic transfection of the gene to the local myocardium, so-called gene therapy.[9]

Pericardiocentesis using the Seldinger maneuver from the subxyphoid to the pericardial space without obvious pericardial effusions is safe[10] and allows the epicardial target to be reached with minimal invasion.[11,12] However, it is difficult to perform the operation within the pericardial space because of numerous obstacles: the coronary vessels, adipose tissue, lung, and phrenic nerves. Therefore, endoscopic guidance is required for the operation. Epicardial biopsy,[13,14] epicardial ablation,[15] pulmonary vein isolation,[16] and implantable cardioverter defibrillator lead placement[17] using pericardial endoscopy have been reported, but risk of injury to arteries, organs, and nerves still remains. The relation among the diameter of the endoscope, material of the sheath, and hemodynamic parameters has not been extensively described. Epicardial inflammation as a chronic effect should be further evaluated. Techniques to obtain a more refined view for critical procedures are not well developed.

From Cardiology,[a] Keio University School of Medicine, Tokyo Japan; and Cardiology,[b] St. Marianna University School of Medicine, Kawasaki, Japan.

Experiments were partially supported by the Japanese Society for Promotion of Science, Grant-in-Aid for Scientific Research, the Ministry of Health, Labor, and Welfare of Japan, and the Suntory Fund for Advanced Cardiac Therapeutics, Keio University School of Medicine. Part of the work was performed at the Keio Research Laboratory Center for Integrated Medical Research.

Disclosures: None.

Received for publication Aug 1, 2010; revisions received Sept 5, 2010; accepted for publication Sept 11, 2010.

Address for reprints: Takehiro Kimura, MD, 35 Shinanomachi Shinjuku-ku Tokyo, Japan 160-8582, Cardiology, Keio University School of Medicine (E-mail: veritas@hp.iij4u.or.jp).

0022-5223/$36.00

doi:10.1016/j.jtcvs.2010.09.050